

Carbon-black combined with TiO₂ and KuQ as sustainable photosystem for a reliable self-powered photoelectrochemical biosensor

Vincenzo Mazzaracchio ^{a,b}, Roberta Marrone ^a, Mattia Forchetta ^a, Federica Sabuzi ^{a,#}, Pierluca Galloni

^a, Mingqing Wang ^c, Ahmet Nazligul ^c, Kwang-Leong Choy ^c, Fabiana Arduini ^{a,d,#}, Danila Moscone ^a

^a Department of Chemical Science and Technologies, University of Rome "Tor Vergata", via della Ricerca Scientifica 1, 00133 Rome, Italy.

^b Okinawa Institute of Science and Technology Graduate University, Micro/Bio/Nanofluidics Unit, 1919-1, Tancha, Onna-son, 904-0495, Okinawa, Japan.

^c Institute for Materials Discovery University College London, Torrington Place, London WC1E 7JE, UK.

^d SENSE4MED, Via della ricerca scientifica, 00133, Rome, Italy

Corresponding authors. E-mail: Fabiana.arduini@uniroma2.it, federica.sabuzi@uniroma2.it

Keywords: modified screen-printed electrodes; carbon black; alcohol dehydrogenase, ethanol.

Abstract

Since our first work published in *Electrochemistry Communication* in 2010 (12, 346-350), many carbon black-(CB) based electrochemical printed (bio)sensors have been reported in the literature, addressing voltammetric and potentiometric measurements. Herein, we report the first photoelectrochemical biosensor based on a printed electrode modified with carbon black. In detail, the photoelectrochemical sensor has been designed by using, in addition to CB, TiO₂ and KuQ dye, because the use of only TiO₂ and CB still requires UV irradiation, while KuQ is characterized by a broad and intense absorption spectrum in the visible region allowing for an easy set-up with a cost-effective portable laser. Once optimized the fabrication and working conditions, namely the solvent for the TiO₂ dispersion (i.e. H₂O/dimethylformamide (1:1 v/v)), the amount of TiO₂/KuQ to cast onto the working electrode surface (i.e. 4 µg), the applied potential (i.e. +0.4 V), and the working solution (i.e. Tris buffer at pH 8.8), the sensor was challenged for NADH measurement obtaining a linear range up to 8 mM and a detection limit, calculated as $3 \sigma_b/\text{slope}$, equal to 20 µM. The subsequent immobilization of alcohol dehydrogenase demonstrated the capability of this biosensor to detect ethanol up to 1 M, with the detection limit equal to 0.062 mM, indicating that the CB-TiO₂/KuQ modification can regenerate the coenzyme even in the immobilized form, with improved analytical

performances in terms of enhancement of the linearity. Finally, ethanol was detected in a real sample, i.e. white wine, with a good recovery value of 91.60 ± 0.01 %, demonstrating the applicability of the developed miniaturized biosensor in white wine samples.

1
2
3
4
5
6
7
8
9
10
11
12
13
14
15
16
17
18
19
20
21
22
23
24
25
26
27
28
29
30
31
32
33
34
35
36
37
38
39
40
41
42
43
44
45
46
47
48
49
50
51
52
53
54
55
56
57
58
59
60
61
62
63
64
65

1. Introduction

The introduction of nanomaterials in the different areas of science has largely modified and improved the output of the research activity, delivering highly performant devices, as in the case of the electrochemical analytical tools. In this regard, Escarpa [1] highlighted how the recent advances in several fields, including nanotechnology, boosted the electroanalysis in a true Renaissance period. Carbon-based nanomaterials, including carbon nanotubes, carbon dots, and graphene, have largely improved the electrochemical detection of a wide range of analytes in terms of high sensitivity, low detection limit, and minimization of electrochemical interferences, as well [2-4]. Among carbon-based nanomaterials, in the last decade, our group has largely exploited the old and cost-effective carbon black (CB) in the design of electrochemical (bio)sensors in the last decade. We demonstrated that the combination of the very low-cost (c.a. 1 €/Kg) CB nanomaterial with a cost-effective printed electrochemical chip (c.a. 1 €/each) allows for the development of sustainable electroanalytical devices with reliable analytical performances and applications in several fields including biomedical, defense, environmental, and agrifood ones, as highlighted in our recent review [5]. Furthermore, the use of CB in the development of electrochemical (bio)sensors has been further enlarged by using this nanomaterial to fabricate different types of electrodes, including the more conventional glassy carbon and carbon paste electrodes as well as voltammetric and potentiometric (bio)sensors. For instance, CB modified printed electrodes have been used for the voltammetric detection of several phenolic compounds, namely catechol, gallic acid, caffeic acid, and tyrosol, by square wave voltammetry with a detection limit of 0.1 μM , 1 μM , 0.8 μM , and 2 μM , respectively, at lower applied potential and with higher sensitivity without fouling problem, when compared with the unmodified printed electrodes [6]. A glassy carbon electrode was used by the Compton's group for nicotine detection by using square wave voltammetry obtaining a detection limit of 12.4 μM at a bare glassy carbon electrode while 2 μM in the case of a CB-modified glassy carbon electrode [7]. Elliott's group

1 highlighted the electrochemical performance and stability of CB modified electrodes when compared
2 with the bare ones using cyclic voltammetry and electrochemical impedance spectroscopy as
3 techniques, observing that the CB-modified electrodes are characterized by long-term stability, i.e.
4 at least six months, and improved electrocatalytic properties compared with unmodified electrode
5 [8]. Thus, in the case of voltammetric sensors, the presence of CB demonstrated its capability to
6 reduce applied potential and to increase the sensitivity, as demonstrated in the case of NADH,
7 cysteine, thiocholine, phosphate, capsaicin, thanks to its key features such as the nano dimensions,
8 the onion-like carbon structure, and the high number of defect sites [9-13]. Otherwise, in the case of
9 a potentiometric sensor like the one developed for sodium detection, we demonstrated that the
10 presence of a CB layer between the working electrode of the printed sensor and the selective
11 membrane avoids the formation of an aqueous layer, improving the potential stability together with
12 good shelf life and resistance to oxygen and light interferences [14]. The different CB features have
13 also been exploited in developing sensors modified with CB-based nanocomposite. The defect sites
14 have been exploited to synthesize Prussian Blue nanoparticles on CB, furnishing a CB-Prussian Blue
15 nanoparticle powder ease to be used as a dispersion to modify the electrode by drop-casting for the
16 hydrogen peroxide detection itself [15, 16] or as the byproduct of the oxidase-based enzymatic
17 reaction [17]. The high surface area has been exploited to load electrochemical mediator by layer-
18 by-layer approach, as in the case of thionine loaded on the previously modified electrode with CB for
19 bisphenol A detection [18] or by loading the electrochemical mediator during the dispersion
20 preparation as in the case of cobalt phthalocyanine, delivering a stable and homogenous dispersion
21 of CB-cobalt phthalocyanine used to fabricate a biosensor for the detection of pesticides [19].
22

23 Another exciting field of research concerns photocatalytic-based systems, where TiO_2 has been
24 widely employed to produce dye-sensitized TiO_2 for the realization of dye-sensitized solar cells [20],
25 smart cleaning surface and electrodes [21, 22], decontamination of pollutants [23], and
26

photoelectrochemical (bio)sensors [24], as well. TiO_2 has been ascribed to achieve a very efficient photocatalytic activity, high stability, and low cost/toxicity, with the only drawback of the necessity of UV irradiation. Various methods have been investigated to improve the photocatalytic behaviour, by combining carbonaceous nanomaterials such as graphene and carbon nanotubes. Although the electrocatalytic activity of CB used as a nanomodifier of the working electrode has been well demonstrated in the literature since 2010, only two articles have reported the effectiveness of CB for the development of analytical photoelectrochemical sensors. In 2020, Li et al. [25] used CB combined with MIL-101(Cr) to develop a new photoelectrochemical sensor for detecting dopamine using differential pulse voltammetry under visible light. The authors highlighted that the presence of CB could work as an electron bridge by combining its large surface area and the photocatalytic property of Metal-Organic frameworks (MOF), allowing for the detection of dopamine with 0.38 nM as the detection limit. In 2021, Hu et al. [26] reported the photoelectrochemical response of the $g\text{-C}_3\text{N}_4/\text{CB}$ nanocomposite for the sensitive and simultaneous detection of Cd^{2+} , Pb^{2+} , and Hg^{2+} , under irradiation with visible light, with detection limits of 2.1, 0.26 and 0.22 nM, respectively. In this case, the authors hypothesized that the combination of CB with $g\text{-C}_3\text{N}_4$ facilitates the efficient detection of toxic heavy metals in solution thanks to the synergistic effects of these nanomaterials (Fig. 1).

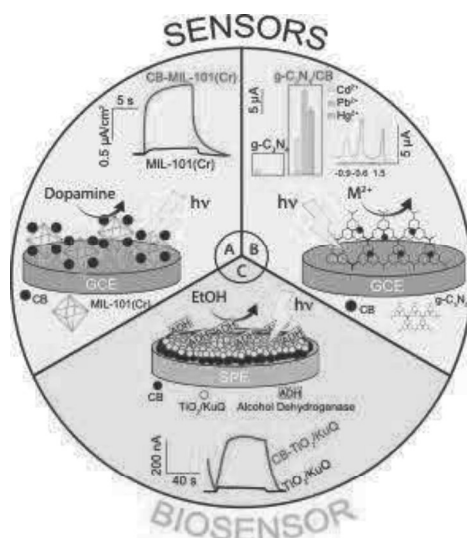


Fig. 1 State of the art of CB-based electrochemical (bio)sensors to develop photoelectrochemical devices. A) CB combined with MIL-101(Cr) for detecting dopamine [25]. B) $g\text{-C}_3\text{N}_4/\text{CB}$ for detecting Cd^{2+} , Pb^{2+} , and Hg^{2+} [26]. C) $\text{TiO}_2/\text{RuO}_4/\text{CB}$ for detecting EtOH [27].

1 C₃N₄/CB nanocomposite-based sensor for simultaneous detection of Cd²⁺, Pb²⁺, and Hg²⁺ [26]. C) The
2 first CB-based photoelectrochemical biosensor developed in this work.
3

4 Herein, we report the first photoelectrochemical biosensor, selecting the NAD-dependent Alcohol
5 Dehydrogenase as an enzyme model, designed by combing CB, TiO₂, and KuQuinone (KuQ) dye to
6 demonstrate an additional feature of CB, namely the enhancement of the photoelectrochemical
7 response due to the retardation of electron-hole pair recombination because of the higher
8 electrochemical conductivity of CB [27]. Furthermore, we reported for the first time the use of the
9 nanocomposite constituted of CB and TiO₂ for sensing applications, further enlarging the application
10 of CB as cost-effective nanomaterial in the electrochemical sensing field.
11
12
13
14
15
16
17
18
19

20 **2. Experimental section**

21 **2.1 Reagents**

22
23 Potassium ferrocyanide (K₄Fe(CN)₆), potassium ferricyanide (K₃Fe(CN)₆), sodium chloride (NaCl),
24 potassium chloride (KCl), phosphate buffer solution (PBS) tablet, Trizma base, *N*-(2-
25 Hydroxyethyl)piperazine-*N*-(2-ethanesulfonic acid) (HEPES), Tetrahydrofuran (THF), Ethanol, *N,N*
26 dimethylformamide (DMF), β-Nicotinamide adenine dinucleotide hydrate (NAD⁺), β-Nicotinamide
27 adenine dinucleotide (NADH), Nafion, Alcohol Dehydrogenase, TiO₂ nanoparticles, 6-bromohexanoic
28 acid, absolute ethanol, diethyl ether, sodium sulfate anhydrous, 2-hydroxy-1,4-naphthoquinone,
29 cesium carbonate (Cs₂CO₃), ferrocene, dimethyl sulfoxide (DMSO), dichloromethane, hexane,
30 pentane, methanol (MeOH), were purchased from Sigma-Aldrich (St. Louise, USA). Carbon Black
31 N220 was obtained from Cabot Corporation (Ravenna, Italy).
32
33
34
35
36
37
38
39
40
41
42
43
44
45
46
47
48
49
50

51 **2.2 Fabrication of screen-printed electrodes**

52
53 Screen-printed electrodes (SPEs) were produced using a 245 DEK (Weymouth, UK) screen-printing
54 machine. A flexible polyester sheet (Autostat HT5), purchased from Autotype Italia (Milan, Italy), was
55 used as the substrate to print the electrodes. Graphite-based ink (Electrodag 423 SS) from Acheson
56
57
58
59
60
61
62
63
64
65

1 (Milan, Italy) was used to print both the working and auxiliary electrodes, while silver/silver chloride
2 ink (Electrodag 6038 SS) to print the pseudo-reference electrode. The resultant diameter of the
3
4
5 working electrode was 0.3 cm with a geometric area equal to 0.07 cm².
6
7
8
9

10 **2.3 Synthesis of ethyl 6-bromohexanoate**

11
12 4.3 g of 6-bromohexanoic acid (22 mmol) were dissolved in 200 ml of absolute ethanol, and 1 ml of
13
14 concentrated HCl solution was added. The reaction was conducted at 40 °C under stirring and
15
16 checked by GC analysis. After 24 hours, the mixture was concentrated, diluted with diethyl ether and
17
18 washed with water. The organic phase was dried over anhydrous sodium sulfate and filtered. The
19
20 solvent was removed under reduced pressure. A pale-yellow liquid was isolated (4.4 g, 20 mmol, 90%
21
22 yield).
23
24
25
26

27
28 ¹H NMR in CDCl₃: δ 1.24–1.25 (t, 3H), δ 1.43–1.54 (m, 2H), δ 1.62–1.72 (m, 2H), δ 1.84–1.94 (m, 2H),
29
30 δ 2.30–2.35 (t, 2H), δ 3.40–3.45 (t, 2H), δ 4.10–4.18 (q, 2H).
31
32
33
34
35

36 **2.4 Synthesis of 1-(3-ethoxycarbonylpropyl)KuQuinone (KuQ3CO₂Et)**

37
38 1 g of 2-hydroxy-1,4-naphthoquinone (5.75 mmol), 2.68 g of ethyl 6-bromohexanoate (12 mmol),
39
40 2.54 g of Cs₂CO₃ (8 mmol), 63 mg of sublimated ferrocene (0.33 mmol) and 22 mL of DMSO were
41
42 mixed at 114 °C, for 41 hours. Afterwards, the reaction mixture was diluted with 100 mL of
43
44 dichloromethane, filtered and washed three times with 400 ml of NaCl saturated aqueous solution.
45
46 The organic phase was dried over anhydrous sodium sulfate, filtered, and the solvent was removed
47
48 under reduced pressure. The product was purified by *plug* chromatography (SiO₂, eluent CH₂Cl₂); the
49
50 purple powder was precipitated from dichloromethane–hexane and then washed with pentane (173
51
52 mg, 0.40 mmol, 14% yield).
53
54
55
56
57
58
59
60
61
62
63
64
65

¹H NMR in CDCl₃: δ 1.23–1.25 (t, 3H), δ 2.04–2.09 (m, 2H), δ 2.47–2.50 (t, 2H), δ 3.50–3.53 (t, 2H), δ 4.11–4.15 (q, 2H), δ 7.71–7.79 (m, 4H), δ 8.22–8.27 (m, 4H), δ 18.20 (s, 1H).

2.5 Synthesis of 1-(3-carboxylpropyl)KuQuinone (KuQ)

45 mg of 1-(3-ethoxycarbonylpropyl)KuQuinone (0.10 mmol) were dissolved in 50 ml of THF and 5 ml of a saturated solution of NaOH in MeOH were added. The system was kept under stirring overnight, at room temperature, and checked by TLC. A purple precipitate was obtained after neutralization with 0.1 M HCl (39.2 mg, 0.095 mmol, 95% yield). UV-vis in THF [λ_{\max} , nm (ϵ , M⁻¹cm⁻¹)]: 565 (15346); 530 (13564).

2.6 Procedure for TiO₂/KuQ nanocomposite fabrication (TiO₂/KuQ nanocomposite)

10 mg of TiO₂ nanoparticles were added to a 3 mL solution of KuQ 0.24 mM in freshly distilled THF. The mixture was stirred for 4 h at RT. After, the obtained suspension was centrifuged four times at 5000 rpm for 3 minutes, discarding each time the supernatant, using a solution of distilled THF for the first two centrifugations and ethanol for the others. Finally, the collected precipitate was left overnight to allow the complete evaporation of solvents.

2.7 Procedure for TiO₂/KuQ dispersion

5 mg of TiO₂/KuQ nanocomposite were dipped in 2.5 mL of dimethylformamide, and then 2.5 mL of water were added. The dispersion was sonicated for 60 min at 59 kHz, obtaining a pink-coloured dispersion.

2.8 Procedure for Carbon Black dispersion

1
2
3
4
5
6
7
8
9
10
11
12
13
14
15
16
17
18
19
20
21
22
23
24
25
26
27
28
29
30
31
32
33
34
35
36
37
38
39
40
41
42
43
44
45
46
47
48
49
50
51
52
53
54
55
56
57
58
59
60
61
62
63
64
65

Carbon black (CB) was dispersed in a mixture of dimethylformamide/water 1:1 v/v, obtaining a final concentration of 1 mg/mL. In detail, 10 mg of CB powder were first dipped in 5 mL of dimethylformamide, and then 5 mL of water were added. The dispersion was sonicated for 60 min at 59 kHz.

2.9 Procedure for SPE modification

SPEs were modified using the drop-casting method by adding on the surface of the working electrode 6 μ L of the dispersion via three successive steps of 2 μ L. After, 4 μ L of TiO₂/KuQ dispersion were drop-cast onto the CB modified working electrode surface (Fig. S3A).

2.10 Preparation of Alcohol Dehydrogenase biosensor

15 μ L of a mixture containing Nafion, NAD⁺, and alcohol dehydrogenase were placed onto the modified working electrode (Fig. S3B). In detail, the mixture was obtained by mixing 100 μ L of Nafion (1 % v/v prepared in water), 100 μ L of NAD⁺ 20 mM, and 100 μ L of enzyme stock solution (1133 U/mL).

2.11 (Photo)electrochemical measurements

Cyclic voltammetry (CV) and amperometry were performed by using the portable potentiostat PalmSens⁴ (Palm Instrument, The Netherlands) connected to a laptop and controlled by PSTrace software.

CV measurements were carried out using a solution of 5 mM ferro/ferricyanide (1:1 v/v) in KCl 0.1 M. For photocurrent measurements, 100 μ L of the analysis solution were cast onto the SPEs, and the working electrode was irradiated by a 5 mW LED laser (SDLaser 303) with a wavelength light equal to 530 nm. In detail, the light was switched on and off every 30 seconds under the external bias of 0.4

1 V applied by the potentiostat. The working solution pH and applied potential were optimized using a
2 50 μM NADH solution, as it is the final product of the alcohol dehydrogenase reaction with ethanol
3 and NAD⁺.
4

5
6
7 80 μL of ethanol solution at different concentrations was cast onto the SPE for ethanol detection.
8
9 Then the working electrode was irradiated with a 5 mV LED laser (SDLaser 303) with a wavelength
10 light equal to 530 nm.
11
12

13
14
15 For real sample analysis, white wine was diluted 1:4 v/v with the working solution, i.e. Tris buffer 0.1
16 M, pH 8.8.
17
18
19
20
21
22

23 **2.12 ATR-FTIR, SEM, and EDX analyses**

24
25 ATR-FTIR spectra were recorded with a FT-IR Nicolet iS50 Thermo Scientific (Madison, WI, USA)
26 spectrometer. LAMBDA 750UV/Vis/NIR Spectrophotometer from PerkinElmer was used to check the
27 light absorption and calculate the bandgap of TiO₂ nps with and without KuQ surface modification. 1
28 mg pure TiO₂/KuQ-sensitized TiO₂ nps were dispersed into a mixture of 1 ml DI water and 1 ml DMF
29 and stirred for 30min to achieve a homogenous dispersion. Then, 200 μl of the dispersion was
30 dropped on cleaned glass slides, and the dried films were used for UV/Vis measurements. The
31 morphology and elemental composition analysis of the surfaces modified with CB and TiO₂/KuQ
32 nanocomposite were characterized by scanning electron microscopy (EVO LS15, ZEISS) equipped with
33 energy-dispersive X-ray spectroscopy (EDX) from Oxford instrument. The prepared samples on the
34 printed electrodes were directly used for SEM to check the surface morphology. For EDX, the powder
35 composed of nanoparticles was dropped directly on carbon tape and compressed into a compact disk
36 to avoid the signal from the Carbon tape during the EDX test.
37
38
39
40
41
42
43
44
45
46
47
48
49
50
51
52
53
54
55
56
57
58
59
60
61
62
63
64
65

3. Results and discussion

In our system, CB is used as a substrate for the deposition of TiO₂, obtaining an optimal contact between the two materials without the involvement of functional groups. To deliver a visible light-based system, KuQ dye has been selected as a photosensitizer for TiO₂ modification. Only TiO₂ and CB still requires UV irradiation, while KuQ is characterized by a broad and intense absorption spectrum in the visible region between 500 and 600 nm (Figure S1) [28].

The choice of KuQs relays on that: i) such quinoid dyes have been recently studied as photosensitizers in photoelectrochemical devices, given their favourable electrochemical and photophysical properties [28, 29] and ii) the terminal hydroxy, carboxylic, or phosphonic acid functionalities introduced in the KuQ structure promote stable and efficient metal oxide binding [30-34]. In our case, the CO₂H anchoring group has been exploited to develop a KuQ-TiO₂ nanocomposite. As reported in Fig. 2, KuQ is promoted to the excited state under light illumination, where it is a strong oxidant; then, it can accept electrons from NADH and oxidize it to NAD⁺. Meanwhile, KuQ⁻ electron is transferred to the conduction band of TiO₂ and subsequently to the CB-modified electrode, following the energy alignment. This process can proceed automatically without an extra power supply.

To confirm the anchoring of KuQ on TiO₂ nanoparticles, an ATR-IR spectroscopy study was carried out. The IR spectrum of the functionalized TiO₂ shows all the characteristic KuQ signals (Fig. 3, Fig. S2), except for the C=O stretching of the carboxylic acid group (at 1706 cm⁻¹ in pure KuQ). Such signal disappears upon adsorption, unambiguously indicating that KuQ anchoring occurs through the carboxylate group [32].

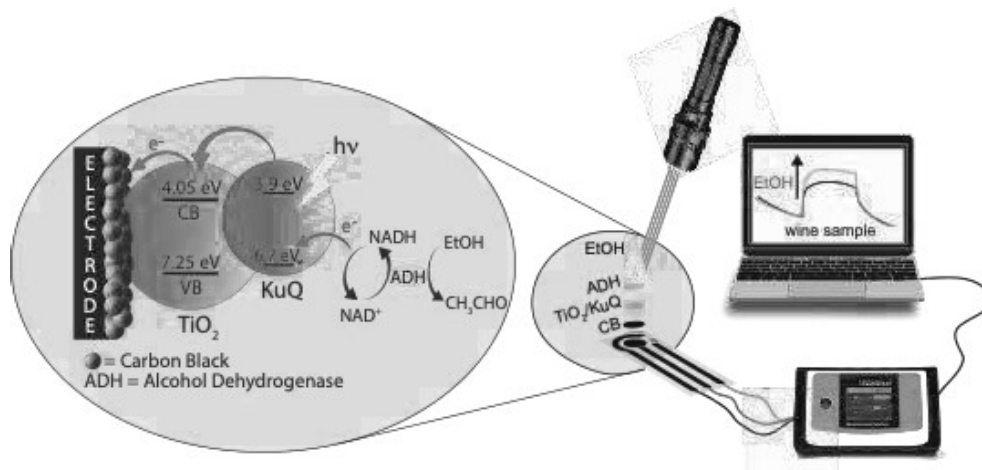


Fig. 2 Scheme of the photoelectrochemical sensing system and the experimental set-up for detection of ethanol.

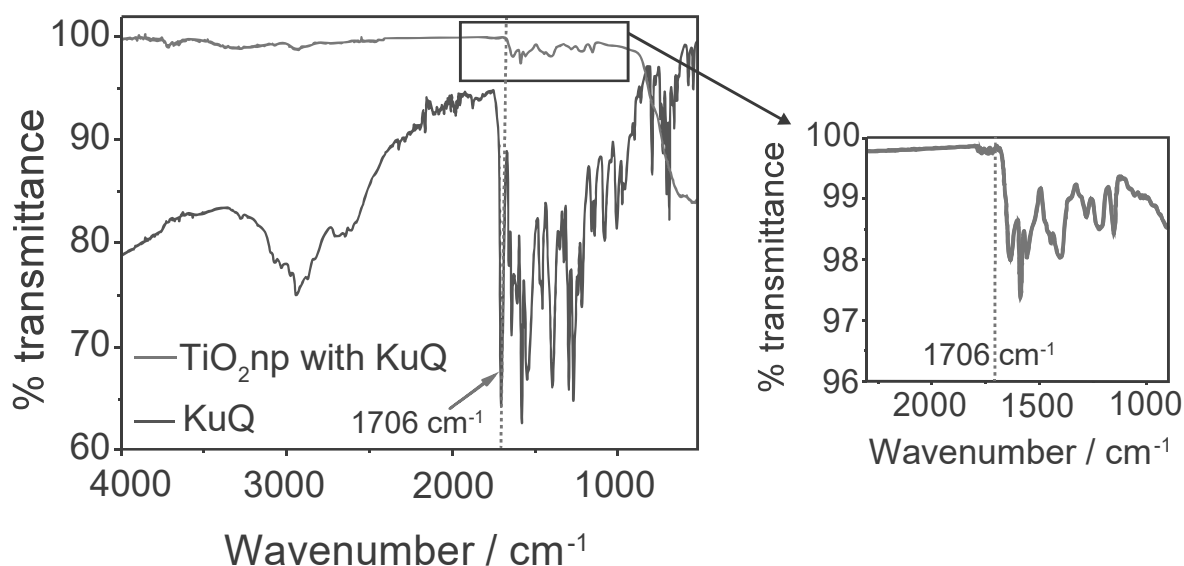


Fig. 3 ATR-IR spectra of CuQ (blue line) and CuQ on TiO₂ nanoparticles (np) (red line). TiO₂ nanoparticle background has been subtracted from the spectrum. Inset: ATR-IR spectrum of CuQ on TiO₂ nanoparticles in the region 2300 – 900 cm⁻¹.

To deliver the photoelectrochemical sensor, screen-printed electrodes (SPEs) were selected as cost-effective and miniaturized electrochemical cells, modified by drop-casting with a first layer of CB dispersion, followed by a second layer with the nanocomposite constituted of TiO₂/CuQ (Figure S3A).

The morphological characterization of the SPEs unmodified (Fig. 4A) and modified with only CB (Fig. 4B), only TiO₂ (Fig. 4C), CB and TiO₂ (Fig. 4D), TiO₂ and CuQ (Fig. 4E), and CB and TiO₂/CuQ (Fig. 4F) is

1 reported at low and high magnification. In detail, in Fig. 4A, the bare SPE shows a webbed surface
2 with irregularly shaped and randomly orientated micrometer-sized flakes of graphite bound together
3
4 with an inert polymeric binder and covered with small particles assigned to the cross-linking agents
5
6 in the original ink [35]. Fig. 4B shows the CB-modified surface, with CB particle sizes ranging from
7
8 around 10 nanometers to 100 nanometers, in agreement with our previous works [13, 35] enabling
9
10 an increase in the surface area of the electrode. Fig. 4C and 4D depict the surfaces modified with TiO_2
11
12 and TiO_2/KuQ . The size of TiO_2 nanoparticles was calculated to be around 21 nm, while the
13
14 implementation with KuQ on the modification does not allow for a clear morphological differentiation
15
16 of the surfaces. To deeply investigate TiO_2 nanoparticles and TiO_2/KuQ nanocomposite, a
17
18 morphological and elemental analysis was performed for TiO_2 nanoparticles and TiO_2/KuQ
19
20 nanocomposite directly deposited onto carbon tape (Fig. 4G, 4H). TiO_2/KuQ nanocomposite (Fig. 4H)
21
22 shows a more homogenous dispersion than pure TiO_2 nanoparticles (Fig. 4G). From the inset EDX
23
24 spectra and element composition, 12.4% of Carbon (C) is detected in TiO_2/KuQ , while the TiO_2
25
26 nanoparticles are composed only of titanium and oxygen.
27
28
29
30
31
32
33
34
35
36
37
38
39
40
41
42
43
44
45
46
47
48
49
50
51
52
53
54
55
56
57
58
59
60
61
62
63
64
65

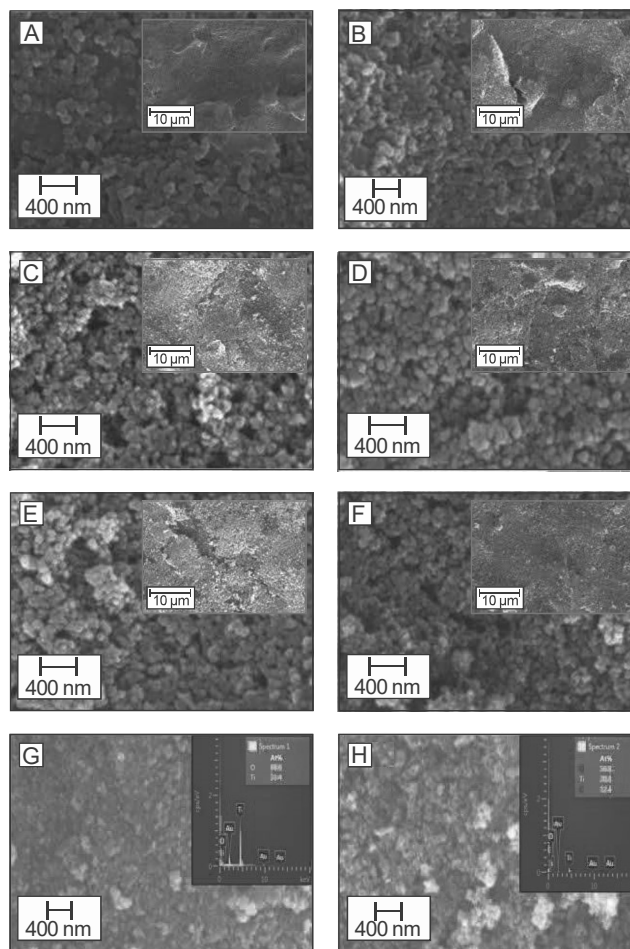


Fig. 4 SEM micrographs of the surface of the working electrode in the case of unmodified SPEs (A) and SPEs modified with CB (B), TiO₂ (C), CB + TiO₂ (D). TiO₂/KuQ nanocomposite (E), and CB + TiO₂/KuQ nanocomposite (F). Inset: images at higher magnification. SEM images and relative EDX spectra for TiO₂ nanoparticles without (G) and with (H) KuQ surface modification.

The photoelectrochemical measurements were firstly carried out using three different configurations of the working electrode, respectively modified with TiO₂/KuQ in the absence (Fig. 5A, red line) and in the presence of CB (Fig. 5A, blue line), to highlight the enhancement of the photoelectrochemical current in the case of working electrode modified with CB. In fact, in the presence of CB, we observe an increase of the photocurrent response of around 15 times, which is much higher than that of the reference sample. In addition, the obtained results are competitive than the ones obtained with glassy carbon-TiO₂ and glassy carbon-graphene/TiO₂ where the photocurrent response is 3.5 times

1 higher [36], demonstrating the suitability of CB as a cheap but performant modifier to improve the
2 charge transport and charge collection in the photoelectrochemical sensing system.
3

4
5 The designed sensor was challenged as a NADH-photoelectrochemical sensor after the optimization
6 of several parameters, including the solvent for the TiO₂ dispersion (i.e. H₂O/DMF (1:1 v/v)) (Fig.
7 S4), the amount of TiO₂/KuQ to cast onto the working electrode surface (i.e. 4 mg) (Fig. S5), the
8 applied potential (i.e. +0.4 V) (Fig. S6), and the working solution (i.e. Tris buffer at pH 8.8) (Fig. 5B). In
9
10 the case of the working solution optimization, we have considered both the pH of the successive
11 enzymatic reaction (alcohol dehydrogenase enzyme which prefers alkaline pH) and the different
12 electrolytes able to work in that pH range, observing the best performances in terms of low blank
13 signal (i.e. in the absence of NADH) and repeatability using Tris buffer at pH 8.8. Thus, this working
14
15 solution was selected for the rest of the work. In the case of applied potential, starting from 0.2 V
16 used in the initial studies, we observed a better signal/noise ratio at an applied potential of 0.4 V vs
17 Ag pseudoreference, thus this value was chosen for the analytical characterization of the (bio)sensor.
18
19
20
21
22
23
24
25
26
27
28
29
30
31
32
33

34 Under optimized conditions, the CB-TiO₂/KuQ-SPEs sensor was applied for NADH detection at
35 different concentrations. A linear correlation between NADH and photocurrent was obtained in the
36 range between 50 μM and 8 mM as reported in Fig. 5C, described by the equation $y = (0.2 \pm 0.1) +$
37 $(0.00450 \pm 0.00003) x$, $R^2 = 0.999$. The detection limit, calculated as $3 \sigma_b/\text{slope}$, resulted equal to 20
38 μM. The developed sensor, when compared with some NADH sensors reported in the literature, is
39 characterized by an easy fabrication process based on a straightforward modification of the working
40 electrode surface, i.e. a simple drop-casting of the modifier's solution, and by a wide linear range
41
42
43
44
45
46
47
48
49
50
51
52 (Table S1).
53
54
55
56
57
58
59
60
61
62
63
64
65

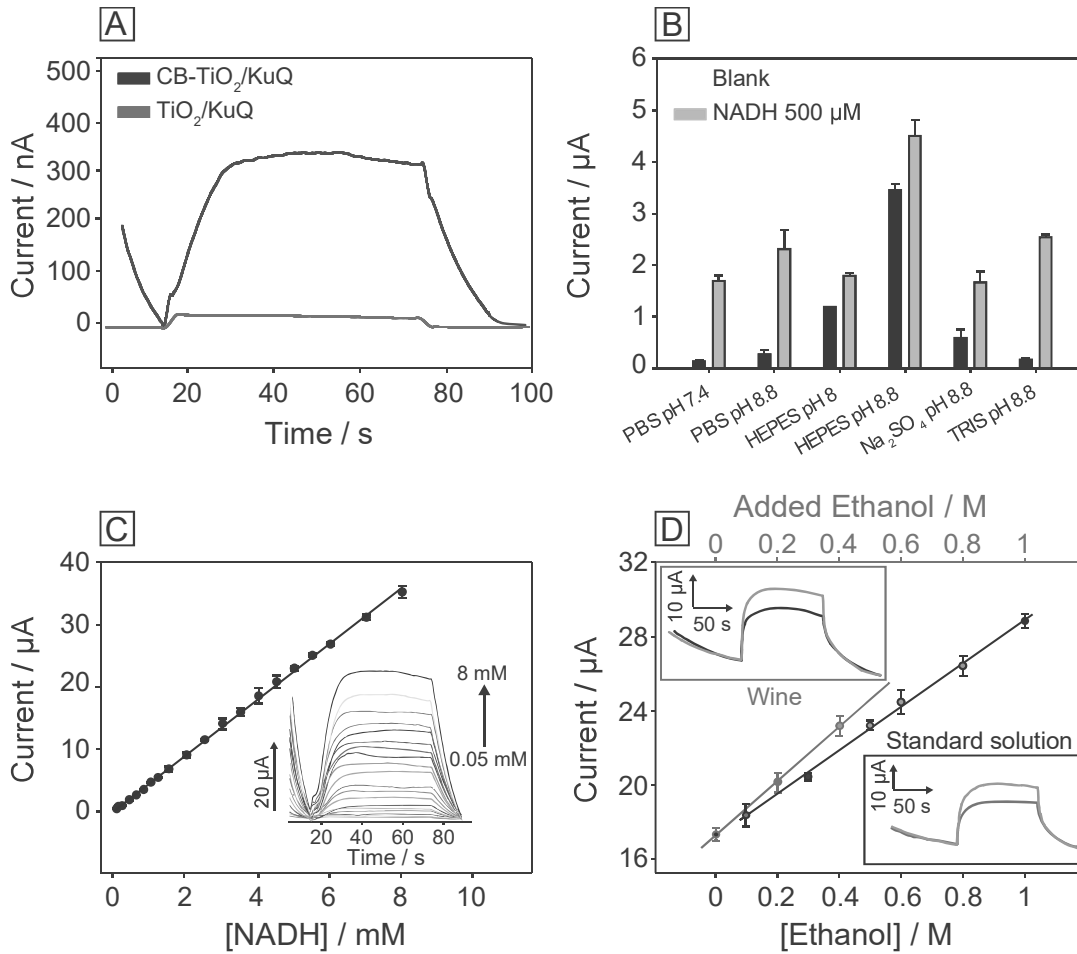


Fig. 5 (A) PEC measurements of NADH 500 μM in PBS pH 7.4, obtained using SPE modified with TiO_2/KuQ nanocomposite, in the absence (red) and presence (blue) of CB, applying a potential of 0.2 V. (B) Histogram bars obtained by PEC measurements using CB- TiO_2/KuQ -SPEs for NADH 500 μM detection in different working solution, applying a potential of 0.2 V. (C) Calibration curve and photocurrent response (inset) at various NADH concentrations using CB- TiO_2/KuQ -SPEs. (D) Calibration curve and photocurrent response (inset) for ethanol (black line) with both NAD^+ and ADH immobilized onto the working electrode, and standard addition method curve and photocurrent response (inset) for quantifying ethanol in diluted wine samples (red line). Applied potential: 0.4 V, working solution: Tris buffer pH 8.8.

Once the sensor was optimized for NADH detection, the suitability of the developed sensor for ethanol detection was assessed by using both the enzyme Alcohol Dehydrogenase and its NAD^+ cofactor immobilized onto the working electrode surface (Fig. S3B) by exploiting the following enzymatic reaction:



1
2
3
4
5 A linear correlation between ethanol and photocurrent was obtained in Tris 0.1 M pH 8.8 standard
6
7 solution, in the range up to 1 M, described by the equation $y = (17.3 \pm 0.2) + (11.6 \pm 0.3) x$, $R^2 = 0.997$
8
9 (Fig. 5D, black curve) with the detection limit equal to 0.062 mM, demonstrating that the CB-
10
11 TiO_2/KuQ modification can regenerate the coenzyme even in the immobilized form, with improved
12
13 analytical performances in terms of enhancement of the linearity (Table S2).
14
15

16
17
18 Finally, to demonstrate the applicability of the developed biosensor, ethanol was detected in a real
19
20 sample, namely white wine. The standard addition method was selected to quantify ethanol in
21
22 diluted wine samples, obtaining the following equation: $y = (17.4 \pm 0.1) + (35.4 \pm 0.4) x$, $R^2 = 0.999$
23
24 (Fig. 5D, red curve). The analysis gave an ethanol concentration equal to 1.96 ± 0.03 M, with a good
25
26 recovery value of 91.60 ± 0.01 %, considering the value stated on the wine label, i.e. 2.14 M.
27
28
29
30

31 32 33 34 35 36 **4. Conclusion**

37
38 Herein, we demonstrated the suitability of CB for the development of photoelectrochemical
39
40 biosensors by using a cost-effective system encompassing printed electrode, portable laser, TiO_2/KuQ
41
42 nanocomposite, and Alcohol Dehydrogenase for the selected target analyte, namely ethanol. The
43
44 high-surface area, the homogeneous dispersion of TiO_2/KuQ nanocomposite on the CB layer, and the
45
46 enhanced electronic transfer of CB due to its higher electrical conductivity, combined with the
47
48 retardation of electron-hole recombination in the presence of TiO_2 nanoparticles, allows for the
49
50 design of novel biosensors, overcoming the state of the art that relegated CB/ TiO_2 just to the
51
52 treatment or degradation of environmental pollutants [37-39]. Worthy of note, the analytical
53
54 performances obtained with the developed NADH sensor open the way for realising any biosensor
55
56
57
58
59
60
61
62
63
64
65

1 combined with other Dehydrogenase enzymes (more than 400), further enlarging the application of
2 cost-effective and reliable screen-printed electrodes modified with CB for electrochemical
3 measurements.
4
5
6
7
8
9

10
11
12 **Acknowledgements** The authors acknowledge support from the Cities partnerships Programme
13 (Rome seed fund) from UCL Global Engagement Office. Prof. Claudia Mazzuca is acknowledged for
14 ATR-IR spectra.
15
16
17
18
19
20
21
22
23
24
25
26
27
28
29
30
31
32
33
34
35
36
37
38
39
40
41
42
43
44
45
46
47
48
49
50
51
52
53
54
55
56
57
58
59
60
61
62
63
64
65

References

- [1] A. Escarpa, Food electroanalysis: sense and simplicity, *Chem. Rec.* 12 (2012)72.
- [2] J. Jose, V. Subramanian, S. Shaji, P.B. Sreeja, An electrochemical sensor for nanomolar detection of caffeine based on nicotinic acid hydrazide anchored on graphene oxide (NAHGO), *Sci. Rep.* 11 (2021) 11662.
- [3] M.N. Norizan, M.H. Moklis, S.Z. Ngah Demon, N.A. Halim, A. Samsuri, I. S. Mohamad, V.F. Knight, N. Abdullah, Carbon nanotubes: Functionalisation and their application in chemical sensors, *RSC Adv.* 10 (2020) 43704.
- [4] S.Tajik, Z. Dourandish, K. Zhang, H. Beitollahi, Q.V. Le, H.W. Jang, M. Shokouhimehr, Carbon and graphene quantum dots: A review on syntheses, characterization, biological and sensing applications for neurotransmitter determination, *RSC Adv.* 10 (2020) 15406.
- [5] F. Arduini, S. Cinti, V. Mazzaracchio, V. Scognamiglio, A. Amine, D. Moscone, Carbon black as an outstanding and affordable nanomaterial for electrochemical (bio) sensor design, *Biosens. Bioelectron.* 156 (2020) 112033.
- [6] D. Talarico, F. Arduini, A. Constantino, M. Del Carlo, D. Compagnone, D. Moscone, G. Palleschi, Carbon black as successful screen-printed electrode modifier for phenolic compound detection, *Electrochem. Commun.* 60 (2015) 78.
- [7] T.W.B. Lo, L. Aldous, R.G. Compton, The use of nano-carbon as an alternative to multi-walled carbon nanotubes in modified electrodes for adsorptive stripping voltammetry, *Sensor. Actuat. B-Chem.* 1 (2012) 361.
- [8] J.K. Nelis, D. Migliorelli, L. Mühlebach, S. Generelli, L. Stewart, C.T. Elliott, K. Campbell, Highly sensitive electrochemical detection of the marine toxins okadaic acid and domoic acid with carbon black modified screen printed electrodes, *Talanta* 228 (2021) 122215.
- [9] S. Cinti, F. Arduini, M. Carbone, L. Sansone, I. Cacciotti, D. Moscone, G. Palleschi, Screen-printed electrodes modified with carbon nanomaterials: a comparison among carbon black, carbon nanotubes and graphene, *Electroanal.* 27 (2015) 2230.
- [10] G. Scordo, D. Moscone, G. Palleschi, F. Arduini, A reagent-free paper-based sensor embedded in a 3D printing device for cholinesterase activity measurement in serum, *Sensor. Actuat. B-Chem.* 258 (2018) 1015.

- 1
2
3
4 [11] D. Talarico, F. Arduini, A. Amine, D. Moscone, G. Palleschi, Screen-printed electrode modified
5 with carbon black nanoparticles for phosphate detection by measuring the electroactive
6 phosphomolybdate complex, *Talanta* 141 (2015) 267.
- 7 [12] P.B. Deroco, O. Fatibello-Filho, F. Arduini, D. Moscone, Electrochemical determination of
8 capsaicin in pepper samples using sustainable paper-based screen-printed bulk modified with carbon
9 black, *Electrochim. Acta* 354 (2020) 136628.
- 10 [13] V. Mazzaracchio, M.R. Tomei, I. Cacciotti, A. Chiodoni, C. Novara, M. Castellino, G. Scordo, A.
11 Amine, D. Moscone, F. Arduini, Inside the different types of carbon black as nanomodifiers for screen-
12 printed electrodes, *Electrochim. Acta* 317 (2019) 673.
- 13 [14] V. Mazzaracchio, A. Serani, L. Fiore, D. Moscone, F. Arduini, All-solid state ion-selective carbon
14 black-modified printed electrode for sodium detection in sweat, *Electrochim. Acta* 394 (2021)
15 139050.
- 16 [15] S. Cinti, F. Arduini, G. Vellucci, I. Cacciotti, F. Nanni, D. Moscone, Carbon black assisted tailoring
17 of Prussian Blue nanoparticles to tune sensitivity and detection limit towards H_2O_2 by using screen-
18 printed electrode, *Electrochem. Commun.* 47 (2014) 63.
- 19 [16] L. Fiore, V. Mazzaracchio, P. Galloni, F. Sabuzi, S. Pezzola, G. Matteucci, D. Moscone, F. Arduini,
20 A paper-based electrochemical sensor for H_2O_2 detection in aerosol phase: Measure of H_2O_2
21 nebulized by a reconverted ultrasonic aroma diffuser as a case of study, *Microchem. J.* 166 (2021)
22 106249.
- 23 [17] N. Colozza, K. Kehe, G. Dionisi, T. Popp, A. Tsoutsoulopoulos, D. Steinritz, D. Moscone, F. Arduini,
24 A wearable origami-like paper-based electrochemical biosensor for sulfur mustard detection,
25 *Biosens. Bioelectron.* 129 (2019) 15.
- 26 [18] M. Portaccio, D. Di Tuoro, F. Arduini, D. Moscone, M. Cammarota, D. G. Mita, M. Lepore, Laccase
27 biosensor based on screen-printed electrode modified with thionine-carbon black nanocomposite
28 for Bisphenol A detection, *Electrochim. Acta* 109 (2013) 340.
- 29 [19] S. Cinti, D. Neagu, M. Carbone, I. Cacciotti, D. Moscone, F. Arduini, Novel carbon black-cobalt
30 phthalocyanine nanocomposite as sensing platform to detect organophosphorus pollutants at
31 screen-printed electrode, *Electrochim. Acta* 188 (2016) 574.
- 32 [20] M. Grätzel, Dye-sensitized solar cells, *J. Photochem. Photobio. C* 4 (2003) 145.
- 33 [21] S.W. Lam, W.Y. Gan, K. Chiang, R. Amal, TiO_2 semiconductor—A smart self-cleaning material, *J.*
34 *Aust. Ceram. Soc.* 44 (2008) 6.
- 35
36
37
38
39
40
41
42
43
44
45
46
47
48
49
50
51
52
53
54
55
56
57
58
59
60
61
62
63
64
65

- 1
2
3
4
5
6
7
8
9
10
11
12
13
14
15
16
17
18
19
20
21
22
23
24
25
26
27
28
29
30
31
32
33
34
35
36
37
38
39
40
41
42
43
44
45
46
47
48
49
50
51
52
53
54
55
56
57
58
59
60
61
62
63
64
65
- [22] V. Pifferi, G. Soliveri, G. Panzarasa, S. Ardizzone, G. Cappelletti, D. Meroni, L. Falciola, Electrochemical sensors cleaned by light: a proof of concept for on site applications towards integrated monitoring systems, *RSC Adv.* 5 (2015) 71210.
- [23] M.E.M. Ali, E.A. Assirey, S.M. Abdel-Moniem, H.S. Ibrahim, Low temperature-calcined TiO₂ for visible light assisted decontamination of 4-nitrophenol and hexavalent chromium from wastewater, *Sci. Rep.* 9 (2019) 19354.
- [24] J. Tang, Y. Wang, J. Li, P. Da, J. Geng, G. Zheng, Sensitive enzymatic glucose detection by TiO₂ nanowire photoelectrochemical biosensors, *J. Mater. Chem. A* 2 (2014) 6153.
- [25] Z. Li, H. Zhang, Q. Zha, C. Zhai, W. Li, L. Zeng, M. Zhu, Photo-electrochemical detection of dopamine in human urine and calf serum based on MIL-101 (Cr)/carbon black, *Microchim. Acta* 187 (2020) 526.
- [26] J. Hu, Z. Li, C. Zhai, L. Zeng, M. Zhu, Photo-assisted simultaneous electrochemical detection of multiple heavy metal ions with a metal-free carbon black anchored graphitic carbon nitride sensor, *Anal. Chim. Acta* 1183 (2021) 338951.
- [27] R. Leary, A. Westwood, Carbonaceous nanomaterials for the enhancement of TiO₂ photocatalysis, *Carbon* 49 (2011) 741.
- [28] F. Sabuzi, S. Lentini, F. Sforza, S. Pezzola, S. Fratelli, O. Bortolini, B. Floris, V. Conte, P. Galloni, KuQuinones equilibria assessment for biomedical applications, *J. Org. Chem.* 82 (2017) 10129.
- [29] F. Valentini, F. Sabuzi, V. Conte, V.N. Nemykin, P. Galloni, Unveiling KuQuinone redox species: an electrochemical and computational cross study, *J. Org. Chem.* 86 (2021) 5680.
- [30] M. Forchetta, V. Conte, G. Fiorani, P. Galloni, F. Sabuzi, A sustainable improvement of ω -bromoalkylphosphonates synthesis to access novel KuQuinones, *Organics* 2 (2021) 107.
- [31] F. Sabuzi, V. Armuzza, V. Conte, B. Floris, M. Venanzi, P. Galloni, E. Gatto, KuQuinones: a new class of quinoid compounds as photoactive species on ITO, *J. Mater. Chem. C* 4 (2016) 622.
- [32] M. Bonomo, F. Sabuzi, A. Di Carlo, V. Conte, D. Dini, P. Galloni, KuQuinones as sensitizers for NiO based p-type dye-sensitized solar cells, *New J. Chem.* 41 (2017) 2769.
- [33] A. Volpato, M. Marasi, T. Gobbato, F. Valentini, F. Sabuzi, V. Gagliardi, A. Bonetto, A. Marcomini, S. Berardi, V. Conte, M. Bonchio, S. Caramori, P. Galloni, A. Sartorel, Photoanodes for water oxidation with visible light based on a pentacyclic quinoid organic dye enabling proton-coupled electron transfer, *Chem. Commun.* 56 (2020) 2248.

- 1
2
3
4
5
6
7
8
9
10
11
12
13
14
15
16
17
18
19
20
21
22
23
24
25
26
27
28
29
30
31
32
33
34
35
36
37
38
39
40
41
42
43
44
45
46
47
48
49
50
51
52
53
54
55
56
57
58
59
60
61
62
63
64
65
- [34] G.A. Volpato, E. Colusso, L. Paoloni, M. Forchetta, F. Sgarbossa, V. Cristino, M. Lunardon, S. Berardi, S. Caramori, S. Agnoli, F. Sabuzi, P. Umari, A. Martucci, P. Galloni, A. Sartorel, Artificial photosynthesis: photoanodes based on polyquinoid dyes onto mesoporous tin oxide surface, *Photochem. Photobiol. Sci.* 20 (2021) 1243.
- [35] F. Arduini, M. Forchielli, A. Amine, D. Neagu, I. Cacciotti, F. Nanni, D. Moscone, G. Palleschi, Screen-printed biosensor modified with carbon black nanoparticles for the determination of paraoxon based on the inhibition of butyrylcholinesterase, *Microchim. Acta* 182 (2015) 643.
- [36] K. Wang, J. Wu, Q. Liu, Y. Jin, J. Yan, J. Cai, Ultrasensitive photoelectrochemical sensing of nicotinamide adenine dinucleotide based on graphene-TiO₂ nanohybrids under visible irradiation, *Anal. Chim. Acta* 745 (2012) 131.
- [37] M.E. Rincon, M.E. Trujillo-Camacho, A.K. Cuentas-Gallegos, N. Casillas, Surface characterization of nanostructured TiO₂ and carbon blacks composites by dye adsorption and photoelectrochemical studies, *Appl. Catal. B-Environ.* 69 (2006) 65.
- [38] C.-C. Mao, H.-S. Weng, Promoting effect of adding carbon black to TiO₂ for aqueous photocatalytic degradation of methyl orange, *Chem. Eng. J.* 155 (2009) 744.
- [39] L. Li, W. Zhu, P. Zhang, Z. Chen, W. Han, Comparison of O₃-BAC, UV/O₃-BAC and TiO₂/UV/O₃-BAC processes for removing organic pollutants in secondary effluents, *Water Res.* 37 (2003) 3646.

Carbon-black combined with TiO₂ and KuQ as sustainable photosystem for a reliable self-powered photoelectrochemical biosensor

Vincenzo Mazzaracchio ^{a,b}, Roberta Marrone ^a, Mattia Forchetta ^a, Federica Sabuzi ^{a,#}, Pierluca Galloni ^a, Mingqing Wang ^c, Ahmet Nazligul ^c, Kwang-Leong Choy ^c, Fabiana Arduini ^{a,d,#}, Danila Moscone ^a

^a Department of Chemical Science and Technologies, University of Rome "Tor Vergata", via della Ricerca Scientifica 1, 00133 Rome, Italy.

^b Okinawa Institute of Science and Technology Graduate University, Micro/Bio/Nanofluidics Unit, 1919-1, Tancha, Onna-son, 904-0495, Okinawa, Japan.

^c Institute for Materials Discovery University College London, Torrington Place, London WC1E 7JE, UK.

^d SENSE4MED, Via della ricerca scientifica, 00133, Rome, Italy

Corresponding authors. E-mail: Fabiana.arduini@uniroma2.it, federica.sabuzi@uniroma2.it

Keywords: modified screen-printed electrodes; carbon black; alcohol dehydrogenase, ethanol.

Abstract

Since our first work published in *Electrochemistry Communication* in 2010 (12, 346-350), many carbon black-(CB) based electrochemical printed (bio)sensors have been reported in the literature, addressing voltammetric and potentiometric measurements. Herein, we report the first photoelectrochemical biosensor based on a printed electrode modified with carbon black. In detail, the photoelectrochemical sensor has been designed by using, in addition to CB, TiO₂ and KuQ dye, because the use of only TiO₂ and CB still requires UV irradiation, while KuQ is characterized by a broad and intense absorption spectrum in the visible region allowing for an easy set-up with a cost-effective portable laser. Once optimized the fabrication and working conditions, namely the solvent for the TiO₂ dispersion (i.e. H₂O/dimethylformamide (1:1 v/v)), the amount of TiO₂/KuQ to cast onto the working electrode surface (i.e. 4 μg), the applied potential (i.e. +0.4 V), and the working solution (i.e. Tris buffer at pH 8.8), the sensor was challenged for NADH measurement obtaining a linear range up to 8 mM and a detection limit, calculated as $3 \sigma_b/\text{slope}$, equal to 20 μM. The subsequent immobilization of alcohol dehydrogenase demonstrated the capability of this biosensor to detect ethanol up to 1 M, with the detection limit equal to 0.062 mM, indicating that the CB-TiO₂/KuQ modification can regenerate the coenzyme even in the immobilized form, with improved analytical

performances in terms of enhancement of the linearity. Finally, ethanol was detected in a real sample, i.e. white wine, with a good recovery value of $91.60 \pm 0.01 \%$, demonstrating the applicability of the developed miniaturized biosensor in white wine samples.

1
2
3
4
5
6
7
8
9
10
11
12
13
14
15
16
17
18
19
20
21
22
23
24
25
26
27
28
29
30
31
32
33
34
35
36
37
38
39
40
41
42
43
44
45
46
47
48
49
50
51
52
53
54
55
56
57
58
59
60
61
62
63
64
65

1. Introduction

The introduction of nanomaterials in the different areas of science has largely modified and improved the output of the research activity, delivering highly performant devices, as in the case of the electrochemical analytical tools. In this regard, Escarpa [1] highlighted how the recent advances in several fields, including nanotechnology, boosted the electroanalysis in a true Renaissance period. Carbon-based nanomaterials, including carbon nanotubes, carbon dots, and graphene, have largely improved the electrochemical detection of a wide range of analytes in terms of high sensitivity, low detection limit, and minimization of electrochemical interferences, as well [2-4]. Among carbon-based nanomaterials, in the last decade, our group has largely exploited the old and cost-effective carbon black (CB) in the design of electrochemical (bio)sensors in the last decade. We demonstrated that the combination of the very low-cost (c.a. 1 €/Kg) CB nanomaterial with a cost-effective printed electrochemical chip (c.a. 1 €/each) allows for the development of sustainable electroanalytical devices with reliable analytical performances and applications in several fields including biomedical, defense, environmental, and agrifood ones, as highlighted in our recent review [5]. Furthermore, the use of CB in the development of electrochemical (bio)sensors has been further enlarged by using this nanomaterial to fabricate different types of electrodes, including the more conventional glassy carbon and carbon paste electrodes as well as voltammetric and potentiometric (bio)sensors. For instance, CB modified printed electrodes have been used for the voltammetric detection of several phenolic compounds, namely catechol, gallic acid, caffeic acid, and tyrosol, by square wave voltammetry with a detection limit of 0.1 μM , 1 μM , 0.8 μM , and 2 μM , respectively, at lower applied potential and with higher sensitivity without fouling problem, when compared with the unmodified printed electrodes [6]. A glassy carbon electrode was used by the Compton's group for nicotine detection by using square wave voltammetry obtaining a detection limit of 12.4 μM at a bare glassy carbon electrode while 2 μM in the case of a CB-modified glassy carbon electrode [7]. Elliott's group

1 highlighted the electrochemical performance and stability of CB modified electrodes when compared
2 with the bare ones using cyclic voltammetry and electrochemical impedance spectroscopy as
3 techniques, observing that the CB-modified electrodes are characterized by long-term stability, i.e.
4 at least six months, and improved electrocatalytic properties compared with unmodified electrode
5 [8]. Thus, in the case of voltammetric sensors, the presence of CB demonstrated its capability to
6 reduce applied potential and to increase the sensitivity, as demonstrated in the case of NADH,
7 cysteine, thiocholine, phosphate, capsaicin, thanks to its key features such as the nano dimensions,
8 the onion-like carbon structure, and the high number of defect sites [9-13]. Otherwise, in the case of
9 a potentiometric sensor like the one developed for sodium detection, we demonstrated that the
10 presence of a CB layer between the working electrode of the printed sensor and the selective
11 membrane avoids the formation of an aqueous layer, improving the potential stability together with
12 good shelf life and resistance to oxygen and light interferences [14]. The different CB features have
13 also been exploited in developing sensors modified with CB-based nanocomposite. The defect sites
14 have been exploited to synthesize Prussian Blue nanoparticles on CB, furnishing a CB-Prussian Blue
15 nanoparticle powder ease to be used as a dispersion to modify the electrode by drop-casting for the
16 hydrogen peroxide detection itself [15, 16] or as the byproduct of the oxidase-based enzymatic
17 reaction [17]. The high surface area has been exploited to load electrochemical mediator by layer-
18 by-layer approach, as in the case of thionine loaded on the previously modified electrode with CB for
19 bisphenol A detection [18] or by loading the electrochemical mediator during the dispersion
20 preparation as in the case of cobalt phthalocyanine, delivering a stable and homogenous dispersion
21 of CB-cobalt phthalocyanine used to fabricate a biosensor for the detection of pesticides [19].
22

23 Another exciting field of research concerns photocatalytic-based systems, where TiO_2 has been
24 widely employed to produce dye-sensitized TiO_2 for the realization of dye-sensitized solar cells [20],
25 smart cleaning surface and electrodes [21, 22], decontamination of pollutants [23], and
26

photoelectrochemical (bio)sensors [24], as well. TiO_2 has been ascribed to achieve a very efficient photocatalytic activity, high stability, and low cost/toxicity, with the only drawback of the necessity of UV irradiation. Various methods have been investigated to improve the photocatalytic behaviour, by combining carbonaceous nanomaterials such as graphene and carbon nanotubes. Although the electrocatalytic activity of CB used as a nanomodifier of the working electrode has been well demonstrated in the literature since 2010, only two articles have reported the effectiveness of CB for the development of analytical photoelectrochemical sensors. In 2020, Li et al. [25] used CB combined with MIL-101(Cr) to develop a new photoelectrochemical sensor for detecting dopamine using differential pulse voltammetry under visible light. The authors highlighted that the presence of CB could work as an electron bridge by combining its large surface area and the photocatalytic property of Metal-Organic frameworks (MOF), allowing for the detection of dopamine with 0.38 nM as the detection limit. In 2021, Hu et al. [26] reported the photoelectrochemical response of the $g\text{-C}_3\text{N}_4/\text{CB}$ nanocomposite for the sensitive and simultaneous detection of Cd^{2+} , Pb^{2+} , and Hg^{2+} , under irradiation with visible light, with detection limits of 2.1, 0.26 and 0.22 nM, respectively. In this case, the authors hypothesized that the combination of CB with $g\text{-C}_3\text{N}_4$ facilitates the efficient detection of toxic heavy metals in solution thanks to the synergistic effects of these nanomaterials (Fig. 1).

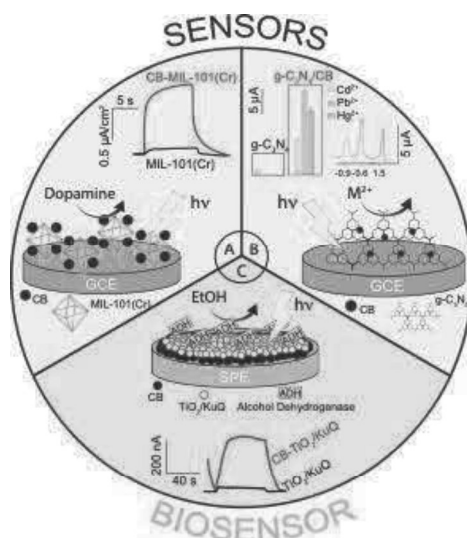


Fig. 1 State of the art of CB-based electrochemical (bio)sensors to develop photoelectrochemical devices. A) CB combined with MIL-101(Cr) for detecting dopamine [25]. B) $g\text{-C}_3\text{N}_4/\text{CB}$ for detecting heavy metal ions [26]. C) $\text{TiO}_2/\text{RuO}_4/\text{CB}/\text{ADH}$ for detecting EtOH [27].

1 C₃N₄/CB nanocomposite-based sensor for simultaneous detection of Cd²⁺, Pb²⁺, and Hg²⁺ [26]. C) The
2 first CB-based photoelectrochemical biosensor developed in this work.
3

4 Herein, we report the first photoelectrochemical biosensor, selecting the NAD-dependent Alcohol
5 Dehydrogenase as an enzyme model, designed by combing CB, TiO₂, and KuQuinone (KuQ) dye to
6 demonstrate an additional feature of CB, namely the enhancement of the photoelectrochemical
7 response due to the retardation of electron-hole pair recombination because of the higher
8 electrochemical conductivity of CB [27]. Furthermore, we reported for the first time the use of the
9 nanocomposite constituted of CB and TiO₂ for sensing applications, further enlarging the application
10 of CB as cost-effective nanomaterial in the electrochemical sensing field.
11
12
13
14
15
16
17
18
19

20 **2. Experimental section**

21 **2.1 Reagents**

22
23 Potassium ferrocyanide (K₄Fe(CN)₆), potassium ferricyanide (K₃Fe(CN)₆), sodium chloride (NaCl),
24 potassium chloride (KCl), phosphate buffer solution (PBS) tablet, Trizma base, *N*-(2-
25 Hydroxyethyl)piperazine-*N*-(2-ethanesulfonic acid) (HEPES), Tetrahydrofuran (THF), Ethanol, *N,N*
26 dimethylformamide (DMF), β-Nicotinamide adenine dinucleotide hydrate (NAD⁺), β-Nicotinamide
27 adenine dinucleotide (NADH), Nafion, Alcohol Dehydrogenase, TiO₂ nanoparticles, 6-bromohexanoic
28 acid, absolute ethanol, diethyl ether, sodium sulfate anhydrous, 2-hydroxy-1,4-naphthoquinone,
29 cesium carbonate (Cs₂CO₃), ferrocene, dimethyl sulfoxide (DMSO), dichloromethane, hexane,
30 pentane, methanol (MeOH), were purchased from Sigma-Aldrich (St. Louise, USA). Carbon Black
31 N220 was obtained from Cabot Corporation (Ravenna, Italy).
32
33
34
35
36
37
38
39
40
41
42
43
44
45
46
47
48
49
50

51 **2.2 Fabrication of screen-printed electrodes**

52
53 Screen-printed electrodes (SPEs) were produced using a 245 DEK (Weymouth, UK) screen-printing
54 machine. A flexible polyester sheet (Autostat HT5), purchased from Autotype Italia (Milan, Italy), was
55 used as the substrate to print the electrodes. Graphite-based ink (Electrodag 423 SS) from Acheson
56
57
58
59
60
61
62
63
64
65

1
2
3
4
5
6
7
8
9
10
11
12
13
14
15
16
17
18
19
20
21
22
23
24
25
26
27
28
29
30
31
32
33
34
35
36
37
38
39
40
41
42
43
44
45
46
47
48
49
50
51
52
53
54
55
56
57
58
59
60
61
62
63
64
65

(Milan, Italy) was used to print both the working and auxiliary electrodes, while silver/silver chloride ink (Electrodag 6038 SS) to print the pseudo-reference electrode. The resultant diameter of the working electrode was 0.3 cm with a geometric area equal to 0.07 cm².

2.3 Synthesis of ethyl 6-bromohexanoate

4.3 g of 6-bromohexanoic acid (22 mmol) were dissolved in 200 ml of absolute ethanol, and 1 ml of concentrated HCl solution was added. The reaction was conducted at 40 °C under stirring and checked by GC analysis. After 24 hours, the mixture was concentrated, diluted with diethyl ether and washed with water. The organic phase was dried over anhydrous sodium sulfate and filtered. The solvent was removed under reduced pressure. A pale-yellow liquid was isolated (4.4 g, 20 mmol, 90% yield).

¹H NMR in CDCl₃: δ 1.24–1.25 (t, 3H), δ 1.43–1.54 (m, 2H), δ 1.62–1.72 (m, 2H), δ 1.84–1.94 (m, 2H), δ 2.30–2.35 (t, 2H), δ 3.40–3.45 (t, 2H), δ 4.10–4.18 (q, 2H).

2.4 Synthesis of 1-(3-ethoxycarbonylpropyl)KuQuinone (KuQ3CO₂Et)

1 g of 2-hydroxy-1,4-naphthoquinone (5.75 mmol), 2.68 g of ethyl 6-bromohexanoate (12 mmol), 2.54 g of Cs₂CO₃ (8 mmol), 63 mg of sublimated ferrocene (0.33 mmol) and 22 mL of DMSO were mixed at 114 °C, for 41 hours. Afterwards, the reaction mixture was diluted with 100 mL of dichloromethane, filtered and washed three times with 400 ml of NaCl saturated aqueous solution. The organic phase was dried over anhydrous sodium sulfate, filtered, and the solvent was removed under reduced pressure. The product was purified by *plug* chromatography (SiO₂, eluent CH₂Cl₂); the purple powder was precipitated from dichloromethane–hexane and then washed with pentane (173 mg, 0.40 mmol, 14% yield).

¹H NMR in CDCl₃: δ 1.23–1.25 (t, 3H), δ 2.04–2.09 (m, 2H), δ 2.47–2.50 (t, 2H), δ 3.50–3.53 (t, 2H), δ 4.11–4.15 (q, 2H), δ 7.71–7.79 (m, 4H), δ 8.22–8.27 (m, 4H), δ 18.20 (s, 1H).

2.5 Synthesis of 1-(3-carboxylpropyl)KuQuinone (KuQ)

45 mg of 1-(3-ethoxycarbonylpropyl)KuQuinone (0.10 mmol) were dissolved in 50 ml of THF and 5 ml of a saturated solution of NaOH in MeOH were added. The system was kept under stirring overnight, at room temperature, and checked by TLC. A purple precipitate was obtained after neutralization with 0.1 M HCl (39.2 mg, 0.095 mmol, 95% yield). UV-vis in THF [λ_{\max} , nm (ϵ , M⁻¹cm⁻¹)]: 565 (15346); 530 (13564).

2.6 Procedure for TiO₂/KuQ nanocomposite fabrication (TiO₂/KuQ nanocomposite)

10 mg of TiO₂ nanoparticles were added to a 3 mL solution of KuQ 0.24 mM in freshly distilled THF. The mixture was stirred for 4 h at RT. After, the obtained suspension was centrifuged four times at 5000 rpm for 3 minutes, discarding each time the supernatant, using a solution of distilled THF for the first two centrifugations and ethanol for the others. Finally, the collected precipitate was left overnight to allow the complete evaporation of solvents.

2.7 Procedure for TiO₂/KuQ dispersion

5 mg of TiO₂/KuQ nanocomposite were dipped in 2.5 mL of dimethylformamide, and then 2.5 mL of water were added. The dispersion was sonicated for 60 min at 59 kHz, obtaining a pink-coloured dispersion.

2.8 Procedure for Carbon Black dispersion

1
2
3
4
5
6
7
8
9
10
11
12
13
14
15
16
17
18
19
20
21
22
23
24
25
26
27
28
29
30
31
32
33
34
35
36
37
38
39
40
41
42
43
44
45
46
47
48
49
50
51
52
53
54
55
56
57
58
59
60
61
62
63
64
65

Carbon black (CB) was dispersed in a mixture of dimethylformamide/water 1:1 v/v, obtaining a final concentration of 1 mg/mL. In detail, 10 mg of CB powder were first dipped in 5 mL of dimethylformamide, and then 5 mL of water were added. The dispersion was sonicated for 60 min at 59 kHz.

2.9 Procedure for SPE modification

SPEs were modified using the drop-casting method by adding on the surface of the working electrode 6 μ L of the dispersion via three successive steps of 2 μ L. After, 4 μ L of TiO₂/KuQ dispersion were drop-cast onto the CB modified working electrode surface (Fig. S3A).

2.10 Preparation of Alcohol Dehydrogenase biosensor

15 μ L of a mixture containing Nafion, NAD⁺, and alcohol dehydrogenase were placed onto the modified working electrode (Fig. S3B). In detail, the mixture was obtained by mixing 100 μ L of Nafion (1 % v/v prepared in water), 100 μ L of NAD⁺ 20 mM, and 100 μ L of enzyme stock solution (1133 U/mL).

2.11 (Photo)electrochemical measurements

Cyclic voltammetry (CV) and amperometry were performed by using the portable potentiostat PalmSens⁴ (Palm Instrument, The Netherlands) connected to a laptop and controlled by PSTrace software.

CV measurements were carried out using a solution of 5 mM ferro/ferricyanide (1:1 v/v) in KCl 0.1 M. For photocurrent measurements, 100 μ L of the analysis solution were cast onto the SPEs, and the working electrode was irradiated by a 5 mW LED laser (SDLaser 303) with a wavelength light equal to 530 nm. In detail, the light was switched on and off every 30 seconds under the external bias of 0.4

1 V applied by the potentiostat. The working solution pH and applied potential were optimized using a
2 50 μM NADH solution, as it is the final product of the alcohol dehydrogenase reaction with ethanol
3 and NAD^+ .
4

5
6
7 80 μL of ethanol solution at different concentrations was cast onto the SPE for ethanol detection.
8
9 Then the working electrode was irradiated with a 5 mV LED laser (SDLaser 303) with a wavelength
10 light equal to 530 nm.
11
12

13
14
15 For real sample analysis, white wine was diluted 1:4 v/v with the working solution, i.e. Tris buffer 0.1
16 M, pH 8.8.
17
18
19
20
21
22

23 **2.12 ATR-FTIR, SEM, and EDX analyses**

24
25 ATR-FTIR spectra were recorded with a FT-IR Nicolet iS50 Thermo Scientific (Madison, WI, USA)
26 spectrometer. LAMBDA 750UV/Vis/NIR Spectrophotometer from PerkinElmer was used to check the
27 light absorption and calculate the bandgap of TiO_2 nps with and without KuQ surface modification. 1
28 mg pure TiO_2 /KuQ-sensitized TiO_2 nps were dispersed into a mixture of 1 ml DI water and 1 ml DMF
29 and stirred for 30min to achieve a homogenous dispersion. Then, 200 μl of the dispersion was
30 dropped on cleaned glass slides, and the dried films were used for UV/Vis measurements. The
31 morphology and elemental composition analysis of the surfaces modified with CB and TiO_2 /KuQ
32 nanocomposite were characterized by scanning electron microscopy (EVO LS15, ZEISS) equipped with
33 energy-dispersive X-ray spectroscopy (EDX) from Oxford instrument. The prepared samples on the
34 printed electrodes were directly used for SEM to check the surface morphology. For EDX, the powder
35 composed of nanoparticles was dropped directly on carbon tape and compressed into a compact disk
36 to avoid the signal from the Carbon tape during the EDX test.
37
38
39
40
41
42
43
44
45
46
47
48
49
50
51
52
53
54
55
56
57
58
59
60
61
62
63
64
65

3. Results and discussion

In our system, CB is used as a substrate for the deposition of TiO₂, obtaining an optimal contact between the two materials without the involvement of functional groups. To deliver a visible light-based system, KuQ dye has been selected as a photosensitizer for TiO₂ modification. Only TiO₂ and CB still requires UV irradiation, while KuQ is characterized by a broad and intense absorption spectrum in the visible region between 500 and 600 nm (Figure S1) [28].

The choice of KuQs relays on that: i) such quinoid dyes have been recently studied as photosensitizers in photoelectrochemical devices, given their favourable electrochemical and photophysical properties [28, 29] and ii) the terminal hydroxy, carboxylic, or phosphonic acid functionalities introduced in the KuQ structure promote stable and efficient metal oxide binding [30-34]. In our case, the CO₂H anchoring group has been exploited to develop a KuQ-TiO₂ nanocomposite. As reported in Fig. 2, KuQ is promoted to the excited state under light illumination, where it is a strong oxidant; then, it can accept electrons from NADH and oxidize it to NAD⁺. Meanwhile, KuQ⁻ electron is transferred to the conduction band of TiO₂ and subsequently to the CB-modified electrode, following the energy alignment. This process can proceed automatically without an extra power supply.

To confirm the anchoring of KuQ on TiO₂ nanoparticles, an ATR-IR spectroscopy study was carried out. The IR spectrum of the functionalized TiO₂ shows all the characteristic KuQ signals (Fig. 3, Fig. S2), except for the C=O stretching of the carboxylic acid group (at 1706 cm⁻¹ in pure KuQ). Such signal disappears upon adsorption, unambiguously indicating that KuQ anchoring occurs through the carboxylate group [32].

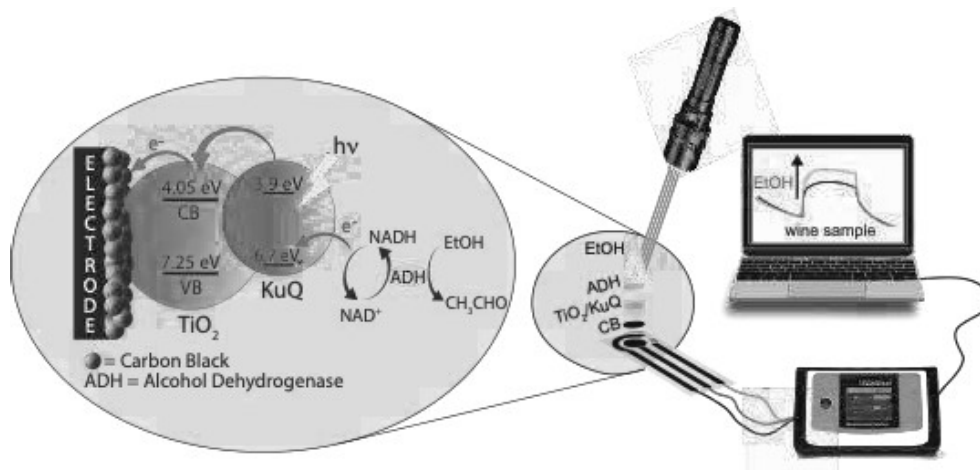


Fig. 2 Scheme of the photoelectrochemical sensing system and the experimental set-up for detection of ethanol.

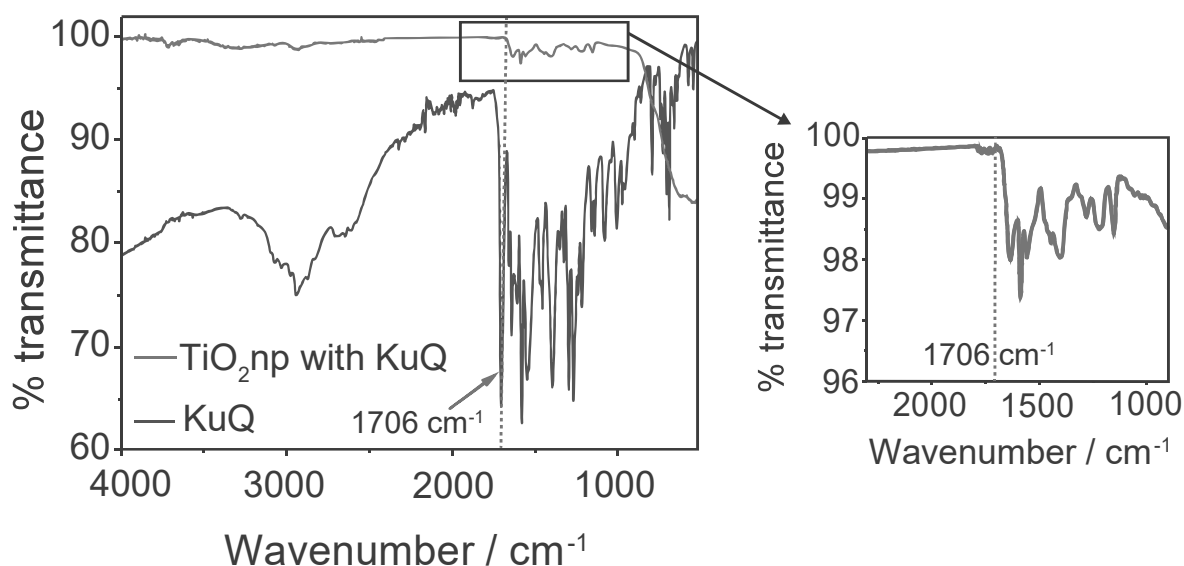


Fig. 3 ATR-IR spectra of KuQ (blue line) and KuQ on TiO_2 nanoparticles (np) (red line). TiO_2 nanoparticle background has been subtracted from the spectrum. Inset: ATR-IR spectrum of KuQ on TiO_2 nanoparticles in the region $2300 - 900 \text{ cm}^{-1}$.

To deliver the photoelectrochemical sensor, screen-printed electrodes (SPEs) were selected as cost-effective and miniaturized electrochemical cells, modified by drop-casting with a first layer of CB dispersion, followed by a second layer with the nanocomposite constituted of TiO_2/KuQ (Figure S3A). The morphological characterization of the SPEs unmodified (Fig. 4A) and modified with only CB (Fig. 4B), only TiO_2 (Fig. 4C), CB and TiO_2 (Fig. 4D), TiO_2 and KuQ (Fig. 4E), and CB and TiO_2/KuQ (Fig. 4F) is

1 reported at low and high magnification. In detail, in Fig. 4A, the bare SPE shows a webbed surface
2 with irregularly shaped and randomly orientated micrometer-sized flakes of graphite bound together
3 with an inert polymeric binder and covered with small particles assigned to the cross-linking agents
4 in the original ink [35]. Fig. 4B shows the CB-modified surface, with CB particle sizes ranging from
5 around 10 nanometers to 100 nanometers, in agreement with our previous works [13, 35] enabling
6 an increase in the surface area of the electrode. Fig. 4C and 4D depict the surfaces modified with TiO₂
7 and TiO₂/KuQ. The size of TiO₂ nanoparticles was calculated to be around 21 nm, while the
8 implementation with KuQ on the modification does not allow for a clear morphological differentiation
9 of the surfaces. To deeply investigate TiO₂ nanoparticles and TiO₂/KuQ nanocomposite, a
10 morphological and elemental analysis was performed for TiO₂ nanoparticles and TiO₂/KuQ
11 nanocomposite directly deposited onto carbon tape (Fig. 4G, 4H). TiO₂/KuQ nanocomposite (Fig. 4H)
12 shows a more homogenous dispersion than pure TiO₂ nanoparticles (Fig. 4G). From the inset EDX
13 spectra and element composition, 12.4% of Carbon (C) is detected in TiO₂/KuQ, while the TiO₂
14 nanoparticles are composed only of titanium and oxygen.
15
16
17
18
19
20
21
22
23
24
25
26
27
28
29
30
31
32
33
34
35
36
37
38
39
40
41
42
43
44
45
46
47
48
49
50
51
52
53
54
55
56
57
58
59
60
61
62
63
64
65

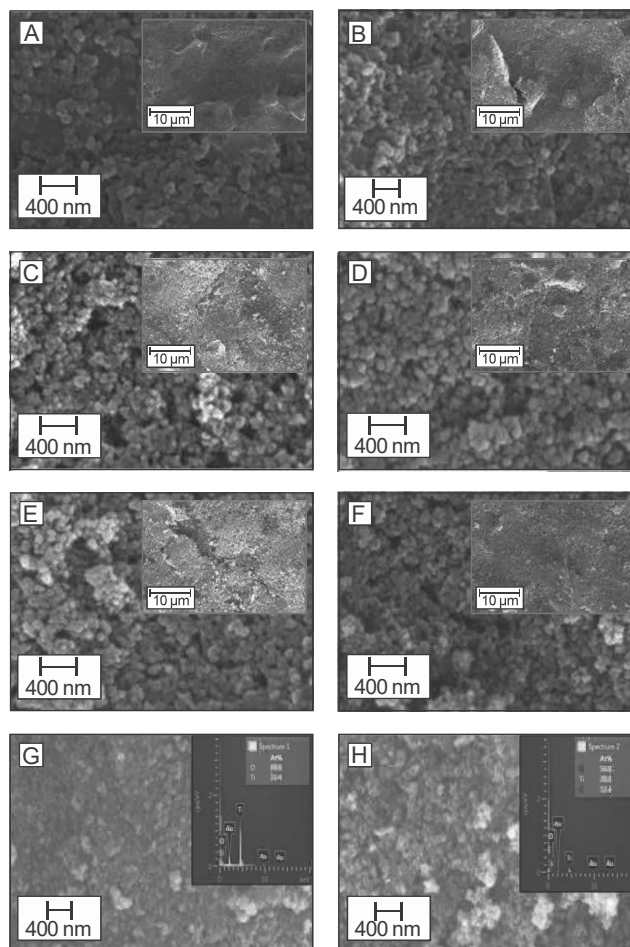


Fig. 4 SEM micrographs of the surface of the working electrode in the case of unmodified SPEs (A) and SPEs modified with CB (B), TiO₂ (C), CB + TiO₂ (D). TiO₂/KuQ nanocomposite (E), and CB + TiO₂/KuQ nanocomposite (F). Inset: images at higher magnification. SEM images and relative EDX spectra for TiO₂ nanoparticles without (G) and with (H) KuQ surface modification.

The photoelectrochemical measurements were firstly carried out using three different configurations of the working electrode, respectively modified with TiO₂/KuQ in the absence (Fig. 5A, red line) and in the presence of CB (Fig. 5A, blue line), to highlight the enhancement of the photoelectrochemical current in the case of working electrode modified with CB. In fact, in the presence of CB, we observe an increase of the photocurrent response of around 15 times, which is much higher than that of the reference sample. In addition, the obtained results are competitive than the ones obtained with glassy carbon-TiO₂ and glassy carbon-graphene/TiO₂ where the photocurrent response is 3.5 times

1 higher [36], demonstrating the suitability of CB as a cheap but performant modifier to improve the
2 charge transport and charge collection in the photoelectrochemical sensing system.
3

4
5 The designed sensor was challenged as a NADH-photoelectrochemical sensor after the optimization
6 of several parameters, including the solvent for the TiO₂ dispersion (i.e. H₂O/DMF (1:1 v/v)) (Fig.
7 S4), the amount of TiO₂/KuQ to cast onto the working electrode surface (i.e. 4 mg) (Fig. S5), the
8 applied potential (i.e. +0.4 V) (Fig. S6), and the working solution (i.e. Tris buffer at pH 8.8) (Fig. 5B). In
9
10 the case of the working solution optimization, we have considered both the pH of the successive
11 enzymatic reaction (alcohol dehydrogenase enzyme which prefers alkaline pH) and the different
12 electrolytes able to work in that pH range, observing the best performances in terms of low blank
13 signal (i.e. in the absence of NADH) and repeatability using Tris buffer at pH 8.8. Thus, this working
14 solution was selected for the rest of the work. In the case of applied potential, starting from 0.2 V
15 used in the initial studies, we observed a better signal/noise ratio at an applied potential of 0.4 V vs
16 Ag pseudoreference, thus this value was chosen for the analytical characterization of the (bio)sensor.
17
18
19
20
21
22
23
24
25
26
27
28
29
30
31
32
33

34 Under optimized conditions, the CB-TiO₂/KuQ-SPEs sensor was applied for NADH detection at
35 different concentrations. A linear correlation between NADH and photocurrent was obtained in the
36 range between 50 μM and 8 mM as reported in Fig. 5C, described by the equation $y = (0.2 \pm 0.1) +$
37 $(0.00450 \pm 0.00003) x$, $R^2 = 0.999$. The detection limit, calculated as $3 \sigma_b/\text{slope}$, resulted equal to 20
38 μM. The developed sensor, when compared with some NADH sensors reported in the literature, is
39 characterized by an easy fabrication process based on a straightforward modification of the working
40 electrode surface, i.e. a simple drop-casting of the modifier's solution, and by a wide linear range
41
42
43
44
45
46
47
48
49
50
51
52 (Table S1).
53
54
55
56
57
58
59
60
61
62
63
64
65

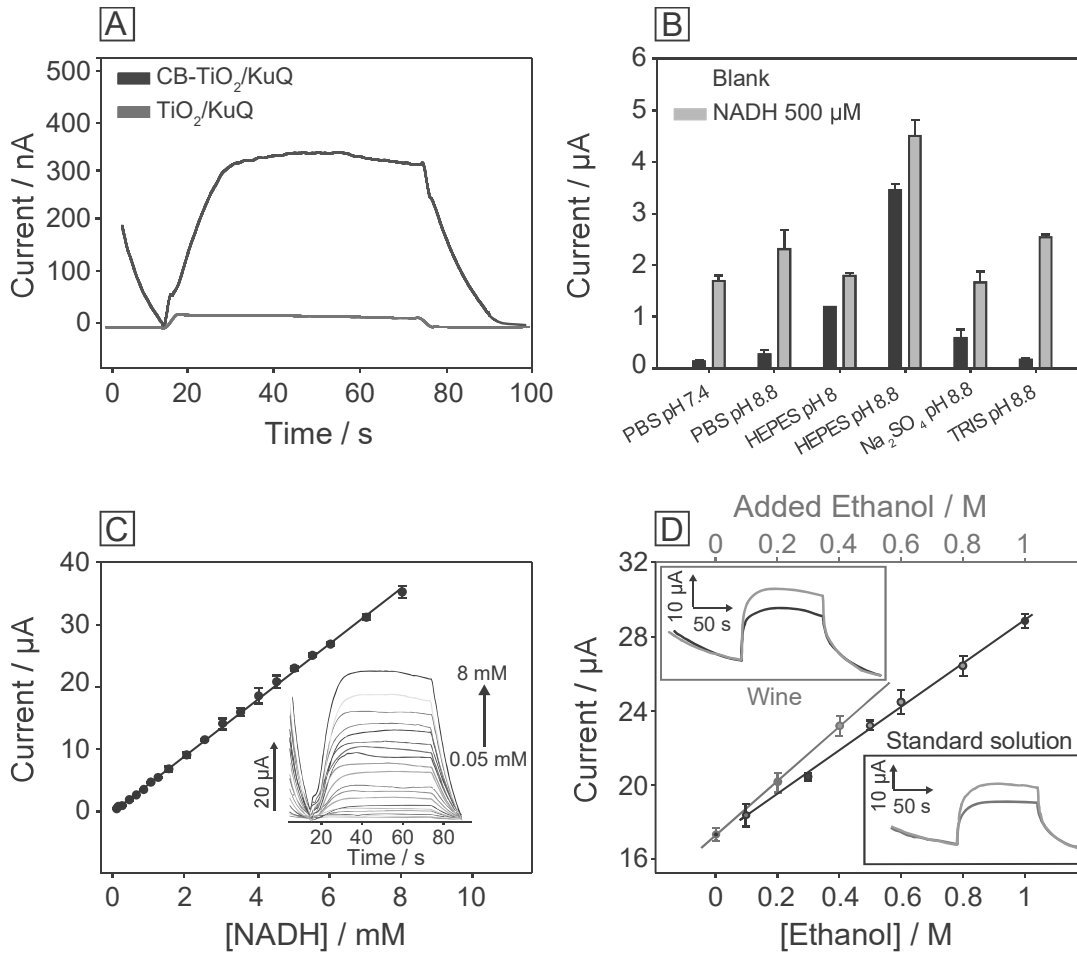


Fig. 5 (A) PEC measurements of NADH 500 μM in PBS pH 7.4, obtained using SPE modified with TiO_2/KuQ nanocomposite, in the absence (red) and presence (blue) of CB, applying a potential of 0.2 V. (B) Histogram bars obtained by PEC measurements using CB- TiO_2/KuQ -SPEs for NADH 500 μM detection in different working solution, applying a potential of 0.2 V. (C) Calibration curve and photocurrent response (inset) at various NADH concentrations using CB- TiO_2/KuQ -SPEs. (D) Calibration curve and photocurrent response (inset) for ethanol (black line) with both NAD^+ and ADH immobilized onto the working electrode, and standard addition method curve and photocurrent response (inset) for quantifying ethanol in diluted wine samples (red line). Applied potential: 0.4 V, working solution: Tris buffer pH 8.8.

Once the sensor was optimized for NADH detection, the suitability of the developed sensor for ethanol detection was assessed by using both the enzyme Alcohol Dehydrogenase and its NAD^+ cofactor immobilized onto the working electrode surface (Fig. S3B) by exploiting the following enzymatic reaction:



1
2
3
4
5 A linear correlation between ethanol and photocurrent was obtained in Tris 0.1 M pH 8.8 standard
6
7 solution, in the range up to 1 M, described by the equation $y = (17.3 \pm 0.2) + (11.6 \pm 0.3) x$, $R^2 = 0.997$
8
9 (Fig. 5D, black curve) with the detection limit equal to 0.062 mM, demonstrating that the CB-
10
11 TiO_2/KuQ modification can regenerate the coenzyme even in the immobilized form, with improved
12
13 analytical performances in terms of enhancement of the linearity (Table S2).
14
15

16
17
18 Finally, to demonstrate the applicability of the developed biosensor, ethanol was detected in a real
19
20 sample, namely white wine. The standard addition method was selected to quantify ethanol in
21
22 diluted wine samples, obtaining the following equation: $y = (17.4 \pm 0.1) + (35.4 \pm 0.4) x$, $R^2 = 0.999$
23
24 (Fig. 5D, red curve). The analysis gave an ethanol concentration equal to 1.96 ± 0.03 M, with a good
25
26 recovery value of 91.60 ± 0.01 %, considering the value stated on the wine label, i.e. 2.14 M.
27
28
29
30

31 32 33 34 35 36 **4. Conclusion**

37
38 Herein, we demonstrated the suitability of CB for the development of photoelectrochemical
39
40 biosensors by using a cost-effective system encompassing printed electrode, portable laser, TiO_2/KuQ
41
42 nanocomposite, and Alcohol Dehydrogenase for the selected target analyte, namely ethanol. The
43
44 high-surface area, the homogeneous dispersion of TiO_2/KuQ nanocomposite on the CB layer, and the
45
46 enhanced electronic transfer of CB due to its higher electrical conductivity, combined with the
47
48 retardation of electron-hole recombination in the presence of TiO_2 nanoparticles, allows for the
49
50 design of novel biosensors, overcoming the state of the art that relegated CB/ TiO_2 just to the
51
52 treatment or degradation of environmental pollutants [37-39]. Worthy of note, the analytical
53
54 performances obtained with the developed NADH sensor open the way for realising any biosensor
55
56
57
58
59
60
61
62
63
64
65

1 combined with other Dehydrogenase enzymes (more than 400), further enlarging the application of
2 cost-effective and reliable screen-printed electrodes modified with CB for electrochemical
3 measurements.
4
5
6
7
8
9

10
11
12 **Acknowledgements** The authors acknowledge support from the Cities partnerships Programme
13 (Rome seed fund) from UCL Global Engagement Office. Prof. Claudia Mazzuca is acknowledged for
14 ATR-IR spectra.
15
16
17
18
19
20
21
22
23
24
25
26
27
28
29
30
31
32
33
34
35
36
37
38
39
40
41
42
43
44
45
46
47
48
49
50
51
52
53
54
55
56
57
58
59
60
61
62
63
64
65

References

- [1] A. Escarpa, Food electroanalysis: sense and simplicity, *Chem. Rec.* 12 (2012)72.
- [2] J. Jose, V. Subramanian, S. Shaji, P.B. Sreeja, An electrochemical sensor for nanomolar detection of caffeine based on nicotinic acid hydrazide anchored on graphene oxide (NAHGO), *Sci. Rep.* 11 (2021) 11662.
- [3] M.N. Norizan, M.H. Moklis, S.Z. Ngah Demon, N.A. Halim, A. Samsuri, I. S. Mohamad, V.F. Knight, N. Abdullah, Carbon nanotubes: Functionalisation and their application in chemical sensors, *RSC Adv.* 10 (2020) 43704.
- [4] S.Tajik, Z. Dourandish, K. Zhang, H. Beitollahi, Q.V. Le, H.W. Jang, M. Shokouhimehr, Carbon and graphene quantum dots: A review on syntheses, characterization, biological and sensing applications for neurotransmitter determination, *RSC Adv.* 10 (2020) 15406.
- [5] F. Arduini, S. Cinti, V. Mazzaracchio, V. Scognamiglio, A. Amine, D. Moscone, Carbon black as an outstanding and affordable nanomaterial for electrochemical (bio) sensor design, *Biosens. Bioelectron.* 156 (2020) 112033.
- [6] D. Talarico, F. Arduini, A. Constantino, M. Del Carlo, D. Compagnone, D. Moscone, G. Palleschi, Carbon black as successful screen-printed electrode modifier for phenolic compound detection, *Electrochem. Commun.* 60 (2015) 78.
- [7] T.W.B. Lo, L. Aldous, R.G. Compton, The use of nano-carbon as an alternative to multi-walled carbon nanotubes in modified electrodes for adsorptive stripping voltammetry, *Sensor. Actuat. B-Chem.* 1 (2012) 361.
- [8] J.K. Nelis, D. Migliorelli, L. Mühlebach, S. Generelli, L. Stewart, C.T. Elliott, K. Campbell, Highly sensitive electrochemical detection of the marine toxins okadaic acid and domoic acid with carbon black modified screen printed electrodes, *Talanta* 228 (2021) 122215.
- [9] S. Cinti, F. Arduini, M. Carbone, L. Sansone, I. Cacciotti, D. Moscone, G. Palleschi, Screen-printed electrodes modified with carbon nanomaterials: a comparison among carbon black, carbon nanotubes and graphene, *Electroanal.* 27 (2015) 2230.
- [10] G. Scordo, D. Moscone, G. Palleschi, F. Arduini, A reagent-free paper-based sensor embedded in a 3D printing device for cholinesterase activity measurement in serum, *Sensor. Actuat. B-Chem.* 258 (2018) 1015.

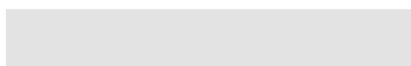
- 1
2
3
4 [11] D. Talarico, F. Arduini, A. Amine, D. Moscone, G. Palleschi, Screen-printed electrode modified
5 with carbon black nanoparticles for phosphate detection by measuring the electroactive
6 phosphomolybdate complex, *Talanta* 141 (2015) 267.
- 7 [12] P.B. Deroco, O. Fatibello-Filho, F. Arduini, D. Moscone, Electrochemical determination of
8 capsaicin in pepper samples using sustainable paper-based screen-printed bulk modified with carbon
9 black, *Electrochim. Acta* 354 (2020) 136628.
- 10 [13] V. Mazzaracchio, M.R. Tomei, I. Cacciotti, A. Chiodoni, C. Novara, M. Castellino, G. Scordo, A.
11 Amine, D. Moscone, F. Arduini, Inside the different types of carbon black as nanomodifiers for screen-
12 printed electrodes, *Electrochim. Acta* 317 (2019) 673.
- 13 [14] V. Mazzaracchio, A. Serani, L. Fiore, D. Moscone, F. Arduini, All-solid state ion-selective carbon
14 black-modified printed electrode for sodium detection in sweat, *Electrochim. Acta* 394 (2021)
15 139050.
- 16 [15] S. Cinti, F. Arduini, G. Vellucci, I. Cacciotti, F. Nanni, D. Moscone, Carbon black assisted tailoring
17 of Prussian Blue nanoparticles to tune sensitivity and detection limit towards H_2O_2 by using screen-
18 printed electrode, *Electrochem. Commun.* 47 (2014) 63.
- 19 [16] L. Fiore, V. Mazzaracchio, P. Galloni, F. Sabuzi, S. Pezzola, G. Matteucci, D. Moscone, F. Arduini,
20 A paper-based electrochemical sensor for H_2O_2 detection in aerosol phase: Measure of H_2O_2
21 nebulized by a reconverted ultrasonic aroma diffuser as a case of study, *Microchem. J.* 166 (2021)
22 106249.
- 23 [17] N. Colozza, K. Kehe, G. Dionisi, T. Popp, A. Tsoutsoulopoulos, D. Steinritz, D. Moscone, F. Arduini,
24 A wearable origami-like paper-based electrochemical biosensor for sulfur mustard detection,
25 *Biosens. Bioelectron.* 129 (2019) 15.
- 26 [18] M. Portaccio, D. Di Tuoro, F. Arduini, D. Moscone, M. Cammarota, D. G. Mita, M. Lepore, Laccase
27 biosensor based on screen-printed electrode modified with thionine-carbon black nanocomposite
28 for Bisphenol A detection, *Electrochim. Acta* 109 (2013) 340.
- 29 [19] S. Cinti, D. Neagu, M. Carbone, I. Cacciotti, D. Moscone, F. Arduini, Novel carbon black-cobalt
30 phthalocyanine nanocomposite as sensing platform to detect organophosphorus pollutants at
31 screen-printed electrode, *Electrochim. Acta* 188 (2016) 574.
- 32 [20] M. Grätzel, Dye-sensitized solar cells, *J. Photochem. Photobio. C* 4 (2003) 145.
- 33 [21] S.W. Lam, W.Y. Gan, K. Chiang, R. Amal, TiO_2 semiconductor—A smart self-cleaning material, *J.*
34 *Aust. Ceram. Soc.* 44 (2008) 6.
- 35
36
37
38
39
40
41
42
43
44
45
46
47
48
49
50
51
52
53
54
55
56
57
58
59
60
61
62
63
64
65

- 1
2
3
4
5
6
7
8
9
10
11
12
13
14
15
16
17
18
19
20
21
22
23
24
25
26
27
28
29
30
31
32
33
34
35
36
37
38
39
40
41
42
43
44
45
46
47
48
49
50
51
52
53
54
55
56
57
58
59
60
61
62
63
64
65
- [22] V. Pifferi, G. Soliveri, G. Panzarasa, S. Ardizzone, G. Cappelletti, D. Meroni, L. Falciola, Electrochemical sensors cleaned by light: a proof of concept for on site applications towards integrated monitoring systems, *RSC Adv.* 5 (2015) 71210.
- [23] M.E.M. Ali, E.A. Assirey, S.M. Abdel-Moniem, H.S. Ibrahim, Low temperature-calcined TiO₂ for visible light assisted decontamination of 4-nitrophenol and hexavalent chromium from wastewater, *Sci. Rep.* 9 (2019) 19354.
- [24] J. Tang, Y. Wang, J. Li, P. Da, J. Geng, G. Zheng, Sensitive enzymatic glucose detection by TiO₂ nanowire photoelectrochemical biosensors, *J. Mater. Chem. A* 2 (2014) 6153.
- [25] Z. Li, H. Zhang, Q. Zha, C. Zhai, W. Li, L. Zeng, M. Zhu, Photo-electrochemical detection of dopamine in human urine and calf serum based on MIL-101 (Cr)/carbon black, *Microchim. Acta* 187 (2020) 526.
- [26] J. Hu, Z. Li, C. Zhai, L. Zeng, M. Zhu, Photo-assisted simultaneous electrochemical detection of multiple heavy metal ions with a metal-free carbon black anchored graphitic carbon nitride sensor, *Anal. Chim. Acta* 1183 (2021) 338951.
- [27] R. Leary, A. Westwood, Carbonaceous nanomaterials for the enhancement of TiO₂ photocatalysis, *Carbon* 49 (2011) 741.
- [28] F. Sabuzi, S. Lentini, F. Sforza, S. Pezzola, S. Fratelli, O. Bortolini, B. Floris, V. Conte, P. Galloni, KuQuinones equilibria assessment for biomedical applications, *J. Org. Chem.* 82 (2017) 10129.
- [29] F. Valentini, F. Sabuzi, V. Conte, V.N. Nemykin, P. Galloni, Unveiling KuQuinone redox species: an electrochemical and computational cross study, *J. Org. Chem.* 86 (2021) 5680.
- [30] M. Forchetta, V. Conte, G. Fiorani, P. Galloni, F. Sabuzi, A sustainable improvement of ω -bromoalkylphosphonates synthesis to access novel KuQuinones, *Organics* 2 (2021) 107.
- [31] F. Sabuzi, V. Armuzza, V. Conte, B. Floris, M. Venanzi, P. Galloni, E. Gatto, KuQuinones: a new class of quinoid compounds as photoactive species on ITO, *J. Mater. Chem. C* 4 (2016) 622.
- [32] M. Bonomo, F. Sabuzi, A. Di Carlo, V. Conte, D. Dini, P. Galloni, KuQuinones as sensitizers for NiO based p-type dye-sensitized solar cells, *New J. Chem.* 41 (2017) 2769.
- [33] A. Volpato, M. Marasi, T. Gobbato, F. Valentini, F. Sabuzi, V. Gagliardi, A. Bonetto, A. Marcomini, S. Berardi, V. Conte, M. Bonchio, S. Caramori, P. Galloni, A. Sartorel, Photoanodes for water oxidation with visible light based on a pentacyclic quinoid organic dye enabling proton-coupled electron transfer, *Chem. Commun.* 56 (2020) 2248.

- 1
2
3
4
5
6
7
8
9
10
11
12
13
14
15
16
17
18
19
20
21
22
23
24
25
26
27
28
29
30
31
32
33
34
35
36
37
38
39
40
41
42
43
44
45
46
47
48
49
50
51
52
53
54
55
56
57
58
59
60
61
62
63
64
65
- [34] G.A. Volpato, E. Colusso, L. Paoloni, M. Forchetta, F. Sgarbossa, V. Cristino, M. Lunardon, S. Berardi, S. Caramori, S. Agnoli, F. Sabuzi, P. Umari, A. Martucci, P. Galloni, A. Sartorel, Artificial photosynthesis: photoanodes based on polyquinoid dyes onto mesoporous tin oxide surface, *Photochem. Photobiol. Sci.* 20 (2021) 1243.
- [35] F. Arduini, M. Forchielli, A. Amine, D. Neagu, I. Cacciotti, F. Nanni, D. Moscone, G. Palleschi, Screen-printed biosensor modified with carbon black nanoparticles for the determination of paraoxon based on the inhibition of butyrylcholinesterase, *Microchim. Acta* 182 (2015) 643.
- [36] K. Wang, J. Wu, Q. Liu, Y. Jin, J. Yan, J. Cai, Ultrasensitive photoelectrochemical sensing of nicotinamide adenine dinucleotide based on graphene-TiO₂ nanohybrids under visible irradiation, *Anal. Chim. Acta* 745 (2012) 131.
- [37] M.E. Rincon, M.E. Trujillo-Camacho, A.K. Cuentas-Gallegos, N. Casillas, Surface characterization of nanostructured TiO₂ and carbon blacks composites by dye adsorption and photoelectrochemical studies, *Appl. Catal. B-Environ.* 69 (2006) 65.
- [38] C.-C. Mao, H.-S. Weng, Promoting effect of adding carbon black to TiO₂ for aqueous photocatalytic degradation of methyl orange, *Chem. Eng. J.* 155 (2009) 744.
- [39] L. Li, W. Zhu, P. Zhang, Z. Chen, W. Han, Comparison of O₃-BAC, UV/O₃-BAC and TiO₂/UV/O₃-BAC processes for removing organic pollutants in secondary effluents, *Water Res.* 37 (2003) 3646.



Click here to access/download
Supplementary Materials
Supplementary materials rev.docx



Credit Author Statement

Mazzaracchio Vincenzo: Conceptualisation of the (bio)sensor, Experimental investigation, electrochemical (bio)sensor fabrication, methodology, data analysis, Writing - review & editing

Roberta Marrone: Experimental investigation

Mattia Forchetta, Federica Sabuzi, Pierluca Galloni: Chemical synthesis and characterization, methodology, data analysis, Writing - review & editing

Mingqing Wang, Ahmet Nazligul, Kwang-Leong Choy: surface characterization, methodology, data analysis, Writing - review & editing

Danila Moscone, Fabiana Arduini: Conceptualisation of the (bio)sensor, Supervision of experiments, Writing - review & editing

Declaration of interests

The authors declare that they have no known competing financial interests or personal relationships that could have appeared to influence the work reported in this paper.

The authors declare the following financial interests/personal relationships which may be considered as potential competing interests: